THE INFLUENCE OF STRESS LEVEL ON THE RATCHETING MAGNITUDE AND PROGRESS RATE IN STEEL ALLOYS UNDER UNIAXIAL LOADING CONDITIONS

By

Prasanth Chandrasekar

Bachelor of Engineering in Aeronautical Engineering

Anna University, Chennai- India, 2014

A report

presented to Ryerson University

in partial fulfillment of the

requirement for the degree of

Master of Engineering

in the Program of

Aerospace Engineering

Toronto, Ontario, Canada, 2016

AUTHOR'S DECLARATION

I hereby declare that I am the sole author of this thesis. This is a true copy of the thesis, including any required final revisions, as accepted by my examiners.

I authorize Ryerson University to lend this thesis to other institutions or individuals for the purpose of scholarly research.

I further authorize Ryerson University to reproduce this thesis by photocopying or by other means, in total or in part, at the request of other institutions or individuals for the purpose of scholarly research.

I understand that my thesis may be made electronically available to the public.

THE INFLUENCE OF STRESS LEVEL ON THE RATCHETING MAGNITUDE AND PROGRESS RATE IN STEEL ALLOYS UNDER UNIAXIAL LOADING CONDITIONS

Master of Engineering in Aerospace Engineering

Ryerson University, Toronto, 2016

Prasanth Chandrasekar, 2016

ABSTRACT

Engineering materials in their service life undergo symmetric or asymmetric fatigue loading, which leads to fatigue damage in the material. Ratcheting damage is due to the application of mean stress under cyclic loading condition. From deformation behavior perspective, application of mean stress under stress-controlled fatigue loading gives rise to accumulation of plastic strain in the material. Ratcheting strain increases with an increase in applied mean stress and stress amplitude. In addition, ratcheting behavior will increase in cyclic damage with the rise in strain accumulation and it can be illustrated by a shift in the hysteresis loop towards large plastic strain amplitudes. This study focuses on the ratcheting behavior of different steel materials under uniaxial cyclic loading condition and suggests a suitable method to arrest ratcheting by loading the materials at zero ratcheting strain rate condition with specified mean stress and stress amplitudes. The three-dimensional surface is created with stress amplitude, mean stress and ratcheting strain rate for different steel materials. This represents a graphical surface zone to study the ratcheting strain rates for various mean stress and stress amplitude combinations.

Keywords: fatigue loading, ratcheting strain, cyclic damage, mean stress and stress amplitudes, plastic strain amplitude, ratcheting strain rate, graphical surface zone.

ACKNOWLEDGEMENTS

After thanking God, I am heartily thankful to my supervisor, Dr. Ahmad Varvani, whose help, guidance and support during my Master’s program provided me with significant knowledge in fatigue analysis. I express my deepest gratitude for his advice, detailed review and constructive comments and criticism during my research. It was a great opportunity to work under his supervision.

Also, I would like to thank my parents, my friends and every person that supported me even with a word.

TABLE OF CONTENTS

LIST OF FIGURES

LIST OF TABLES

LIST OF APPENDICES

NOMENCLATURES

$\overline{a}$	=	Total backstress tensor
$\overline{b}$	=	Second kinematic variable in Bower's hardening rule
C	=	Material constant in the A-F, Bower and the modified hardening rules
dp	=	Increment of equivalent plastic strain
$d\overline{s}$	=	Deviatoric stress increment
$d\overline{\varepsilon}$	=	Total strain increment
$d\overline{\varepsilon}^{p}$	=	Plastic strain increment
$d\overline{\varepsilon}^{e}$	=	Elastic strain increment
E	=	Elastic modulus
G	=	Shear modulus
H_p	=	Plastic modulus function
I	=	Unit tensor
$\overline{n}$	=	Unit exterior normal to the present yield surface at the stress state
$\overline{s}$	=	Deviatoric stress tensor
γ	=	Material constant in the A-F hardening rule
γ_1	=	1st feedback rate of the Bower's model and the modified hardening rule
γ_2,δ	=	Stress level-dependent coefficients in the modified hardening rule
ε_r	=	Ratcheting strain
α	=	Ratcheting strain rate
$\overline{\sigma}$	=	Stress tensor
σ_2	=	Stress amplitude
σ_m	=	Mean stress
σ_a	=	Amplitude stress
σ_y	=	Yield stress
υ	=	Poisson's ratio

CHAPTER 1

Problem Definition and Introduction

1.1 Problem Definition

Ratcheting behavior is seen in all engineering materials subjected to cyclic loading with mean stress. Due to this ratcheting action, the estimated fatigue life of the component reduces, and the life of the material decreases from its estimated life span, so the ratcheting strain needs to be reduced as much as possible to increase component life.

1.2 Introduction

Engineering components in their service life undergo symmetric fatigue loading or asymmetric fatigue loading. Most fatigue damage is greatly influenced by mean stress. From deformation behavior perspective, application of mean stress under stress-controlled fatigue loading gives rise to ratcheting action, which results in accumulation of plastic strain during low cycle fatigue loading [1]. Ratcheting effect not only produces the large deformation but also the fatigue damage in the material; this reduces the life of material. Fatigue life of the material degrades due to the accumulation of ratcheting strain, as shown by the Coffin Mansion Relation. For the past few years, several experiments and simulations have been done to study the degradation of the material due to material nature and imposed stress parameters [2]. Hence in design and structural component assessments of a material, ratcheting-fatigue interaction is more significant due to ratcheting-fatigue failure of material due to cyclic stress loading on the material.

1.3 Ratcheting Assessment

The uniaxial ratcheting behavior of different steel materials were examined with different mean stress (σ_m) and different stress amplitude (σ_a) combinations at room temperature. Ratcheting strains at the different stages were investigated at various types of loading cycles. The schematic triphasic trend of ratcheting strain over stress cycles is shown in Fig. 1.1.

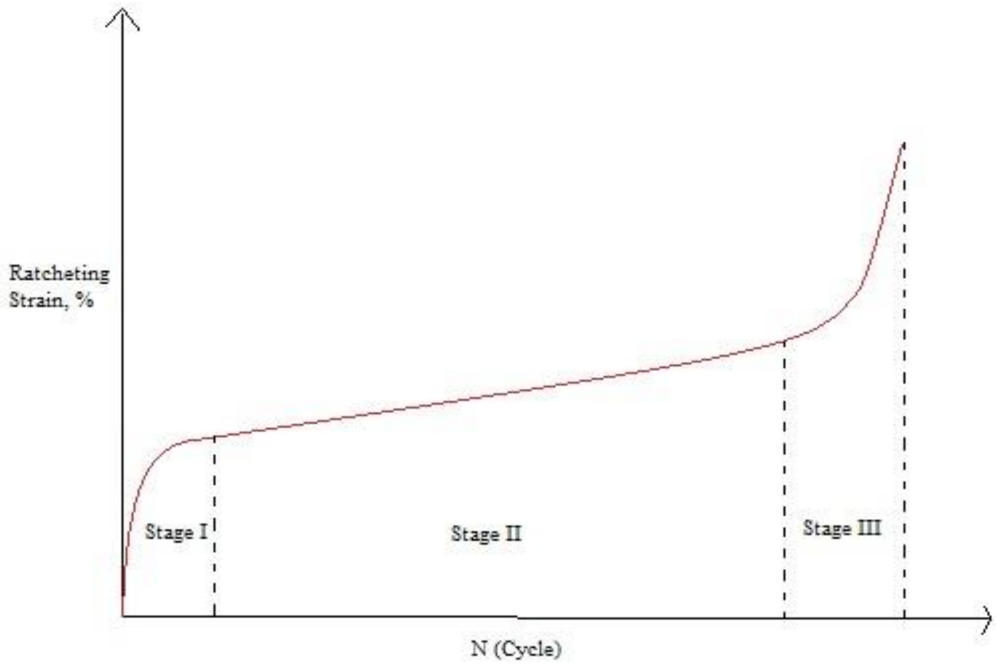

Fig.1.1: Schematic triphasic trend of ratcheting strain over a stress cycles [6].

CHAPTER 2

Materials and Testing Method

2.1 Introduction

The present thesis mainly focuses on uniaxial ratcheting behavior in stage II of different steels, such as interstitial free steel, 16MnR steel, SS304 stainless steel, 42CrMo steel alloy, SS316L steel, 20 CS steel, 1020 steel, SA 333 Gr6C-Mn steel, and HC340LA steel alloy.

2.2 Experimental Ratcheting Test

The ratcheting behavior of a material under uniaxial or multi-axial cyclic loading for different mean and amplitude stresses have been studied in many scholarly journals. The steel specimen used to study the ratcheting behavior is made into a solid cylindrical bar of 10 mm diameter and 30 mm gauge length. Before the material is cyclically tested, the tensile test is performed to study the fundamental properties of the material used for cyclic loadings, such as elastic modulus and yield strength. Ratcheting testing is carried out on electro-hydraulic servo fatigue testing machine. The mechanical loading process is performed in a controlled manner, and experimental data are gathered by the teststar control system that is attached to the testing machine [4]. The axial strain is measured using a strain extensometer of certain limit (i.e., 10% - 50%). The specimen geometry for ratcheting test is shown in Fig. 2.1.

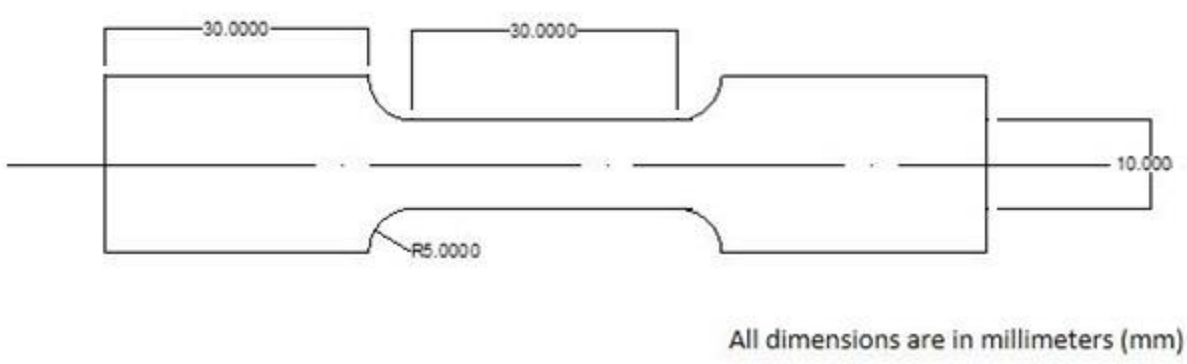

Fig.2.1: Specimen geometry for ratcheting test [5].

Based on the test controlled, testing can be classified into two categories that are as follows (i) constant mean stress with varying stress amplitude (ii) constant stress amplitude with varying mean stress. An example of schematic loading path for ratcheting test as shown in Fig. 2.2.

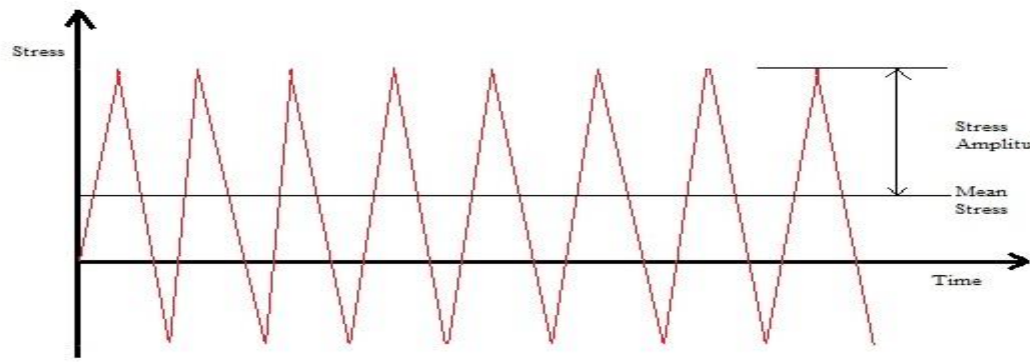

Fig.2.2: schematic loading path for ratcheting test [2].

Ratcheting stain (ε_r) is defined as the average of maximum and minimum strain obtained using extensometer and ε_r given by

$$\varepsilon_r = (\varepsilon_{max} + \varepsilon_{min})/2 \tag{2.1}$$

From the Eq. 2.1, we can find the ratcheting rate $d\varepsilon_r/dN$ after each cycle is calculated, where N is number of cycles. Ratcheting stain effect on fatigue life of the material is investigated by testing the material under uniaxial cyclic stress at room temperature with various mean stress and stress amplitude till the failure occurs. For example Table 2.1 shows the range of mean stress and stress amplitude to study the ratcheting behavior in interstitial free steel [2].

Table 2.1: Mean stress and stress amplitude for ratcheting test in interstitial free (IF) steel [2].

Serial number	σ_m (MPa)	σ_a(MPa)
1	10	130,140,150
2	20	130,140,150
3	30	130,140,150

From the Table 2.1 it is clear that material is subjected to three different types of loading with constant stress amplitude (130,140and 150 MPa) and varying mean stress (10, 20 and 30 MPa).

2.3 Accumulation of Ratcheting Strain

The accumulation of ratcheting strain takes place when the material is subjected to asymmetric cyclic loading with some mean stress values. The nature of the hysteresis loop varies based on the level of imposed mean stress.

From the stress-strain curve for IF steel shown by k. Dutta *et al.*, that with varying mean stress of 10, 20 and 30 MPa and constant stress amplitude of 140 MPa for 100 cycles, it is clear that the hysteresis loop shifts towards the positive plastic strain with the increase in applied mean stress. Plastic strain magnitude for the above figure with the mean stress of 10, 20 and 30 MPa is 3.6%, 5.3% and 6.1%. The similar experiment is performed for different steels and steel alloys with different mean stress and stress amplitude for the different number of cycles.

Ratcheting strain with that of number loading cycles for IF steel is shown in the Fig. 2.3. The increase in loading cycles will result in an increase in accumulation of ratcheting strain for any σ_m and σ_a combinations.

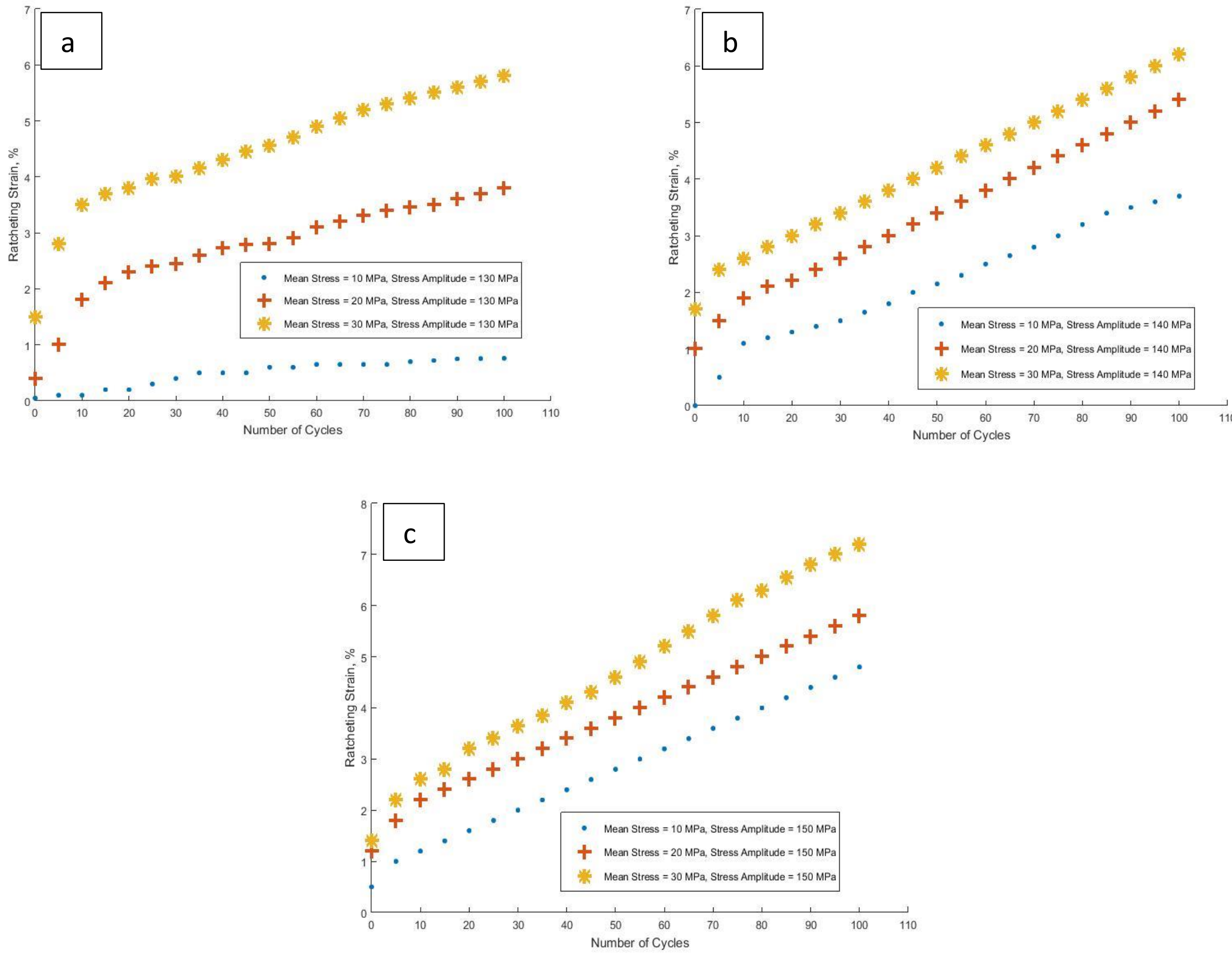

Fig. 2.3: Various ratcheting strains with 100 loading cycles for different mean stress and constant stress amplitudes of (a) 130 MPa (b) 140 MPa (c) 150 MPa in IF steel [2].

From Fig. 2.3 it is clear that ratcheting strain increases with increases in applied mean stress and amplitude stress. Similarly, we can study the ratcheting behaviour of the material by keeping mean stress as constant and varying the stress amplitude as shown in Fig. 2.4.

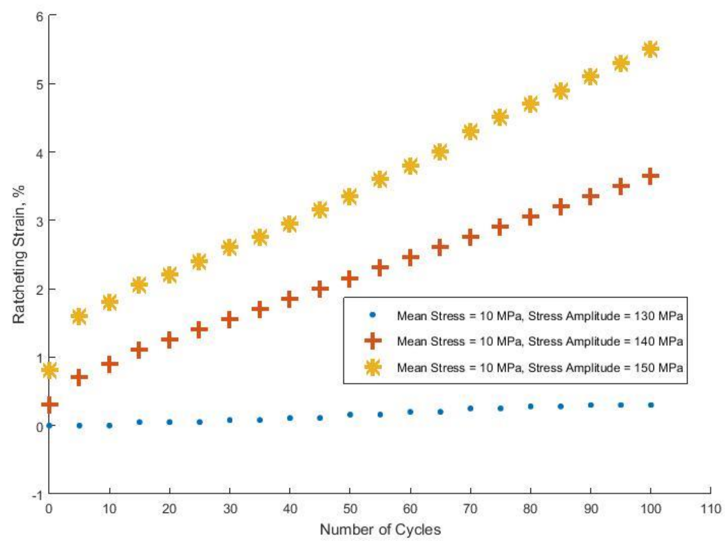

Fig. 2.4: Various ratcheting strains with 100 loading cycles for different stress amplitude and constant mean stress of 10 MPa and varying stress amplitude of 130, 140 and 150 MPa in IF steel [2].

CHAPTER 3

Mathematical Models for Ratcheting Strain Prediction

3.1 Parametric triphasic ratcheting equation

Accumulation of ratcheting strain over three stages of material lifespan is formulated [8]. The ratcheting response of different materials over a stress cycles N_f is expressed as follows

$$\varepsilon_r = \alpha\left(A\left(\frac{\ln N}{\ln N_f} + C\left(\frac{N}{N_f} - \frac{\ln N}{\ln N_f}\right)\right) + B^2\,\frac{\ln\left(1-\frac{N}{N_f}\right)}{\ln\frac{1}{N_f}}\right) \tag{3.1}$$

where the coefficients *A, B, C* and α *are*

$$A = 2\ln\left(\frac{\sigma_y}{E}\right)^{-1} \tag{3.2}$$

$$B = \ln\left(\frac{\Delta\sigma}{E}\right) \tag{3.3}$$

$$C = \frac{1}{2}\left(1 - \frac{\sigma_m}{\Delta\sigma}\right)^{\frac{1}{2n}} \tag{3.4}$$

$$\alpha = \left(\frac{\sigma_{ult}}{\sigma_y}\right)^n \tag{3.5}$$

From the equation above the term $\Delta\sigma$ is the stress range, $2\sigma_a$.

Eq. 3.1 represents the triphasic ratcheting strain accumulation over certain life cycles of the material as shown in the Fig. 3.1. This equation represents the three different stages of ratcheting strain rate. In stage I the ratcheting strain rate drops while in stage II it remains steady and in Stage III it is found that there is a sudden increase in ratcheting strain rate that leads to failure.

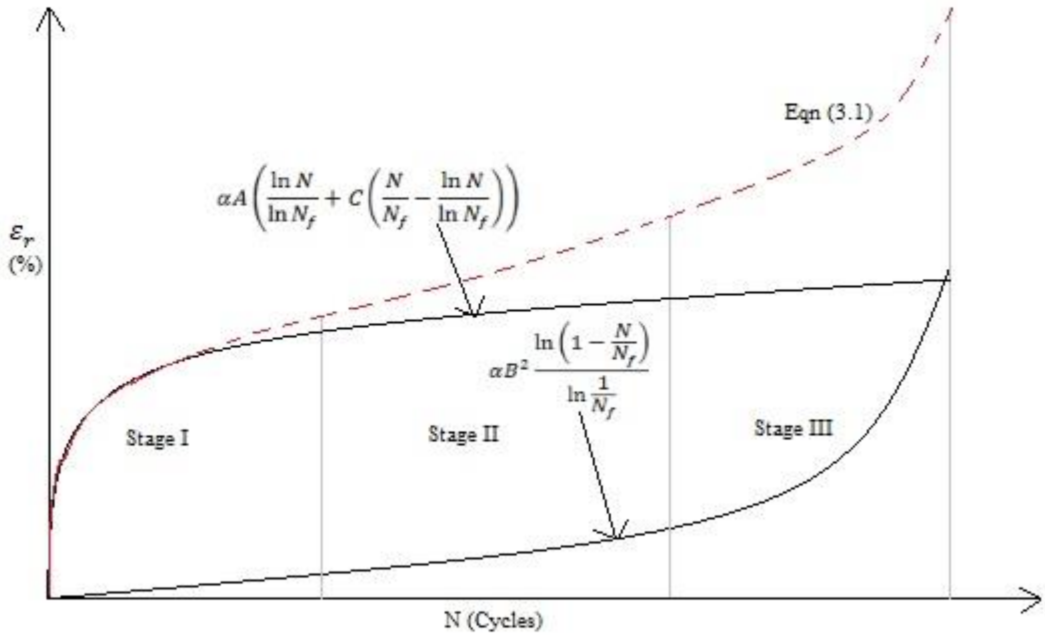

Fig. 3.1: Parametric triphasic ratcheting strain over N_f [8].

3.2 Hardening rule

The theory of cyclic plasticity is based on the strain increment due to elastic and plastic strain components [17], and it can be represented as

$$d\bar{\varepsilon} = d\bar{\varepsilon}^e + d\bar{\varepsilon}^p \tag{3.6}$$

From hooks law, the elastic part is explained as

$$\bar{\varepsilon}^e = \frac{\bar{\sigma}}{2G} - \frac{\upsilon}{E}(\bar{\sigma}.\bar{I})\bar{I} \tag{3.7}$$

Plastic part is defined as the

$$d\bar{\varepsilon}^p = \frac{1}{H_p}(d\bar{s}.\bar{n})\bar{n} \tag{3.8}$$

Where $d\overline{s}$, H_p and $\overline{n}$ are deviatoric stress tensor increment, plastic modulus and normal vector. Deviatoric stress is expressed as

$$\overline{s} = \overline{\sigma} - \frac{1}{3}(\overline{\sigma}.\overline{I})\overline{I} \tag{3.9}$$

Yield surface remain unchanged during loading and unloading conditions. Von-Mises yielding criteria is used

$$f(\overline{s}, \overline{a}, \sigma_y) = \frac{3}{2}(\overline{s} - \overline{a}).(\overline{s} - \overline{a}) - \sigma_y^2 = 0 \tag{3.10}$$

Under the stressed plastic deformation, yield surface movement direction is dictated by the hardening rule.

A nonlinear hardening model is developed by Armstrong-Frederick [12] as

$$d\overline{a} = C\, d\overline{\varepsilon}^p - \gamma\overline{a}\, dp \tag{3.11}$$

where

$$dp = \sqrt{d\overline{\varepsilon}^p . d\overline{\varepsilon}^p} \tag{3.12}$$

C and γ are material constants of strain-controlled uniaxial stress-strain hysteresis loop.

The first term in the Eq. (3.11) refers to strain hardening and second term is nonlinear trend in hardening rule. Plastic modulus function is defined as

$$H_p = C - \gamma(\overline{a}.\overline{n}) \tag{3.13}$$

The ratcheting response in A-F model was overestimating hence Bower modified A-F model to predict ratcheting strain rate and was defined as Bower's hardening rule

$$d\overline{a} = C\, d\overline{\varepsilon}^p - \gamma_1(\overline{a} - \overline{b})dp \tag{3.14}$$

where

$$d\overline{b} = \gamma_2(\overline{a} - \overline{b})dp \tag{3.15}$$

This rule consists of three variables C, γ_1 and γ_2 as material constant, first feedback rate to control the stress-strain hysteresis loop and second feedback rate to determine the ratcheting rate. But Bower's ratcheting rule experienced ratcheting arrest and premature plastic shakedown and hence it is limited by the number of cycles and not beyond the stage I.

Ahmadzadeh and Varvani-Farahani extended the bower's rule to study the ratcheting response of the material under long range of loading cyclic in stage I and II and it is named as A-V model.

$$d\overline{a} = C\ d\overline{\varepsilon}^{p} - \gamma_1(\ \overline{a} - \delta\overline{b})dp \tag{3.16}$$

$$d\overline{b} = \gamma_2(\ \overline{a} - \overline{b})dp \tag{3.17}$$

A new term δ is introduced to avoid ratcheting arrest in stage II as shown in fig. 3.3.
The coefficient γ_2 and δ is expressed as

$$\gamma_2 = \sqrt{\sigma_m}(\sigma_a - \sigma_y)^{\rho_1} + K(\sigma_a - \sigma_y)^{\rho_2} \tag{3.18}$$

$$\delta = 1 - Fe^{\lambda\sigma_a} \tag{3.19}$$

where ρ_1 and ρ_2 and K are material constants. ρ_1 relates to mean stress level and ρ_2 remains unchanged for steels.

CHAPTER 4

Results and Discussion

4.1 Introduction

This thesis focuses only on ratcheting behaviour of different steels at stage II due to uniaxial loading. Ratcheting strain rate is calculated using the tangent of ratcheting strain and loading cycle graph as shown in Fig. 4.1.

$$\textit{Ratcheting strain rate} = \textit{Angular tangent}\ (a/b) = d\varepsilon_r/dN = \alpha \tag{4.1}$$

Hence from the above, the formula ratcheting strain rate for different material at different mean stress and stress amplitude is obtained.

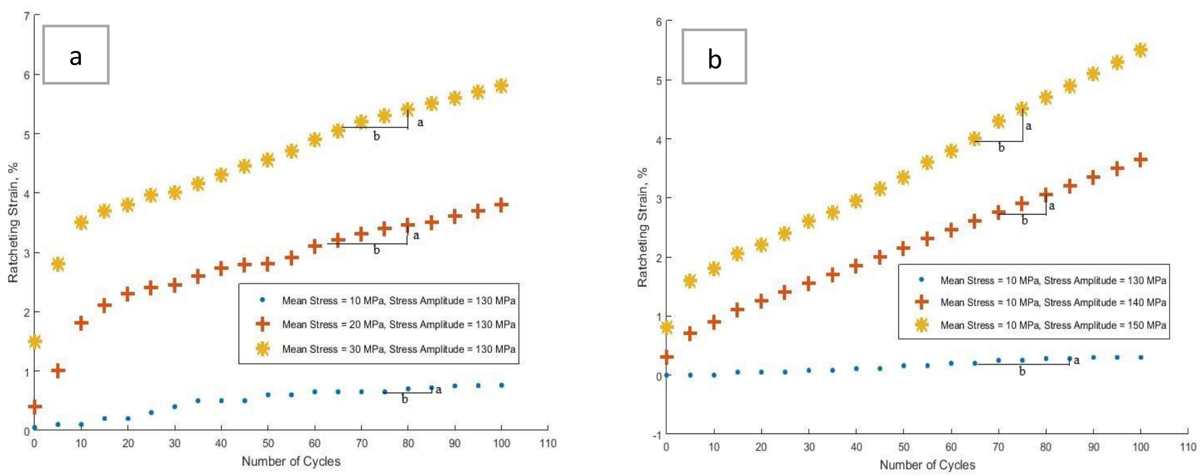

Fig. 4.1: Slope of a /b represent the ratcheting stain rate for IF steel for (a) constant stress amplitude of 130 MPa with varying mean stress (b) constant mean stress of 10 MPa with varying stress amplitude [2].

4.2 Ratcheting strain rate at stage II

From the above value of ratcheting strain rate in different steel materials, I just plotted different sets of graphs for ratcheting strain rate vs. varying mean stress at constant stress amplitude conditions and ratcheting strain rate vs. varying stress amplitude at constant mean stress conditions.

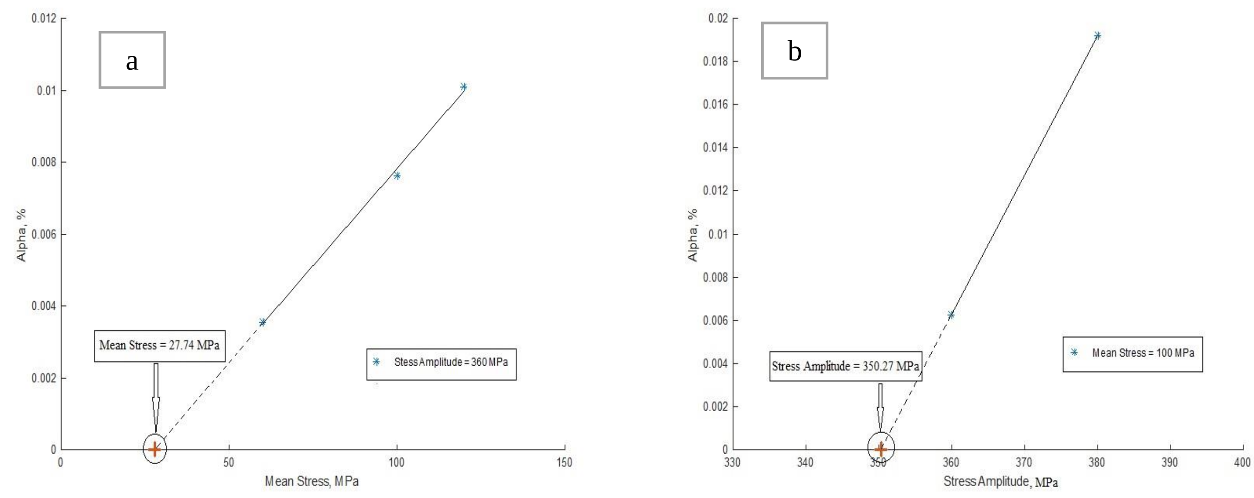

Fig. 4.2: (a) Ratcheting strain rate vs. mean stress at constant stress amplitude of 360 MPa (b) ratcheting strain rate vs. stress amplitude at constant mean stress of 100 MPa is plotted for 16MnR steel.

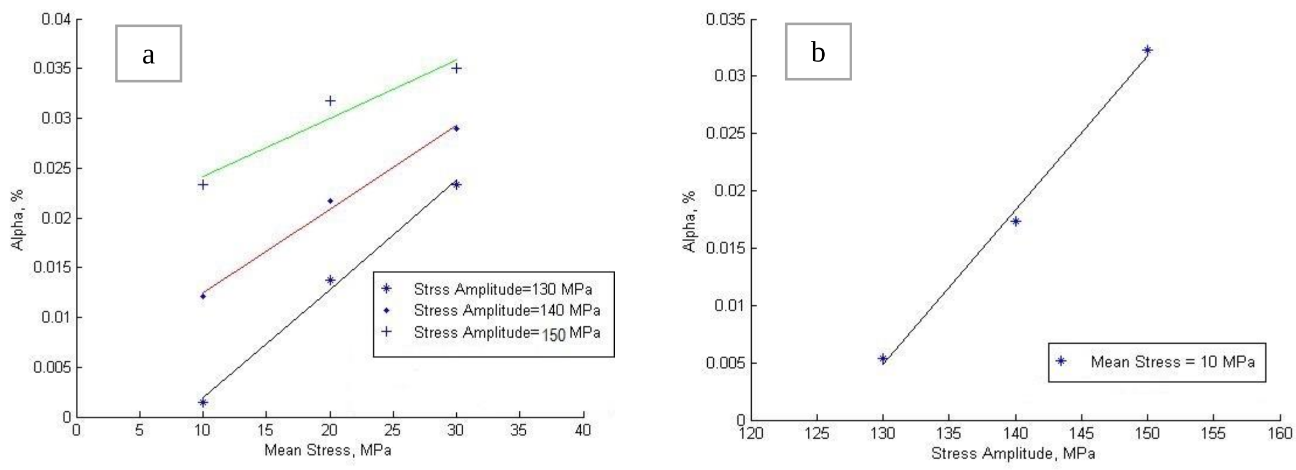

Fig. 4.3: (a) Ratcheting strain rate vs. mean stress at constant stress amplitude of 130, 140 and 150 MPa (b) ratcheting strain rate vs. stress amplitude at constant mean stress of 10 MPa is plotted for interstitial free steel.

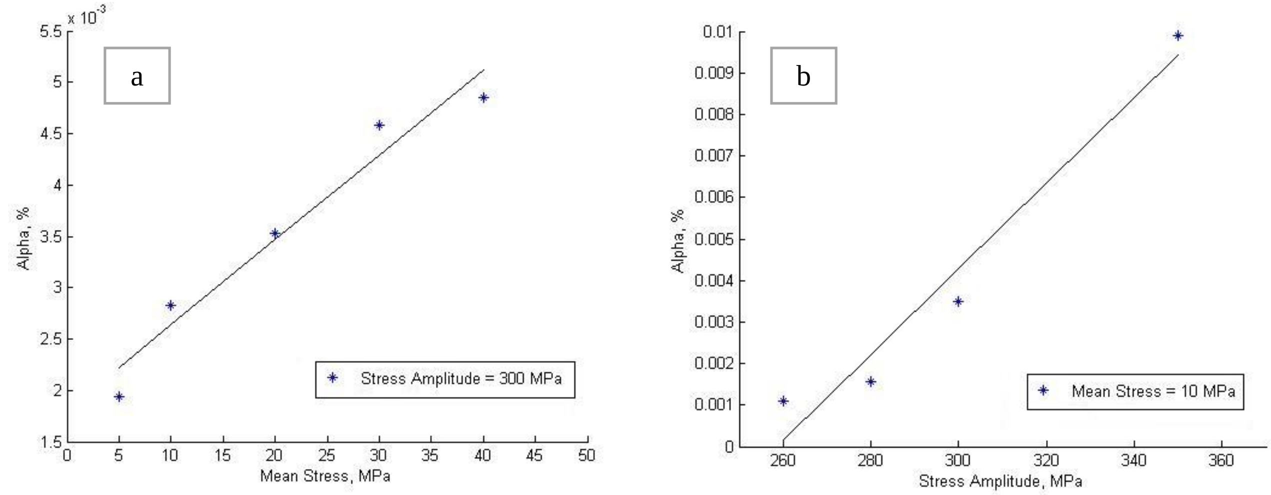

Fig. 4.4: (a) Ratcheting strain rate vs. mean stress at constant stress amplitude of 300 MPa (b) ratcheting strain rate vs. stress amplitude at constant mean stress of 10 MPa is plotted for SS304.

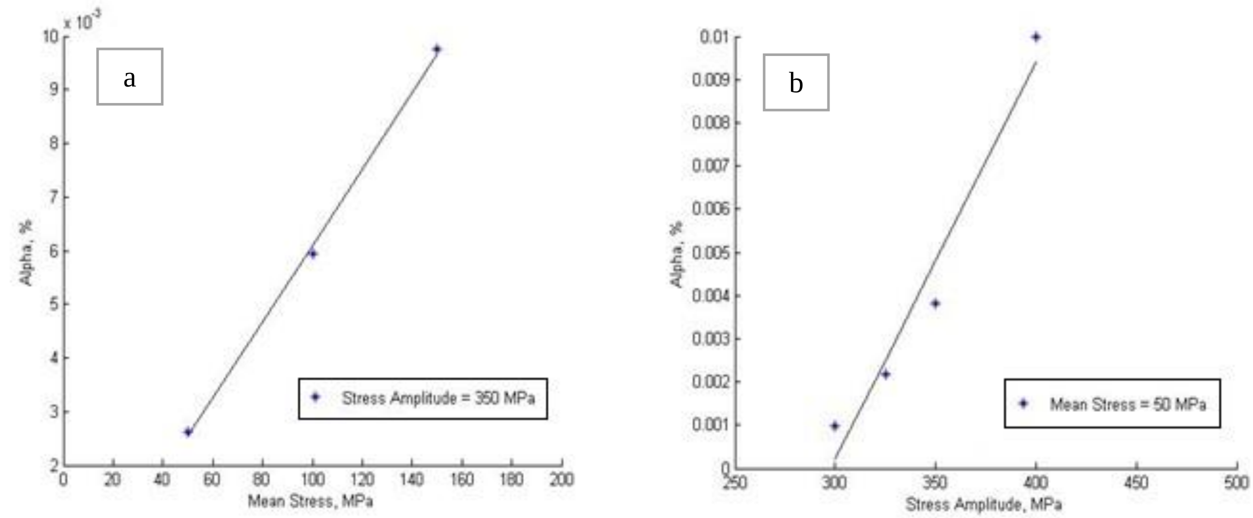

Fig. 4.5: (a) Ratcheting strain rate vs. mean stress at constant stress amplitude of 350 MPa (b) ratcheting strain rate vs. stress amplitude at constant mean stress of 50 MPa is plotted for 42CrMo steel.

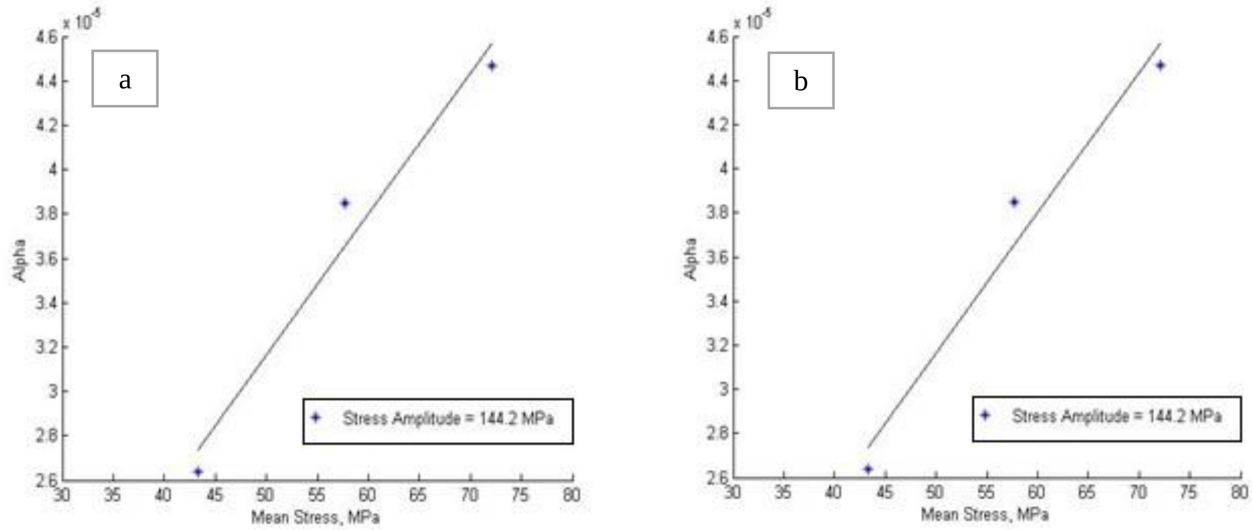

Fig. 4.6: (a) Ratcheting strain rate vs. mean stress at constant stress amplitude of 144.2 MPa (b) ratcheting strain rate vs. stress amplitude at constant mean stress of 28.84 MPa is plotted for titanium-stabilized steel.

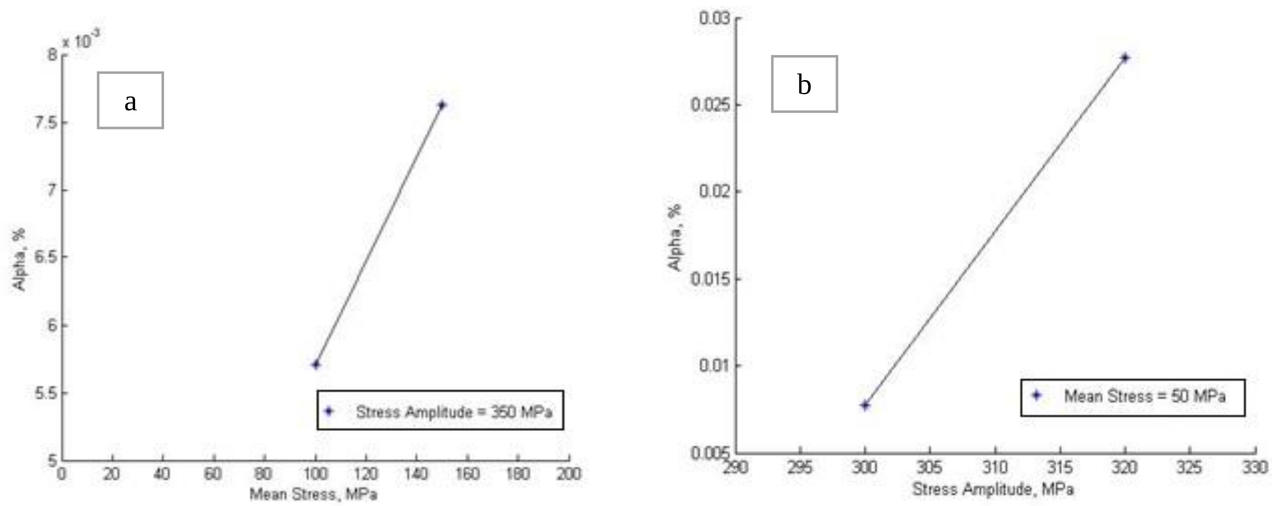

Fig. 4.7: (a) Ratcheting strain rate vs. mean stress at constant stress amplitude of 350 MPa is plotted for 42CrMo steel (b) ratcheting strain rate vs. stress amplitude at constant mean stress of 50 MPa is plotted for 1020 steel.

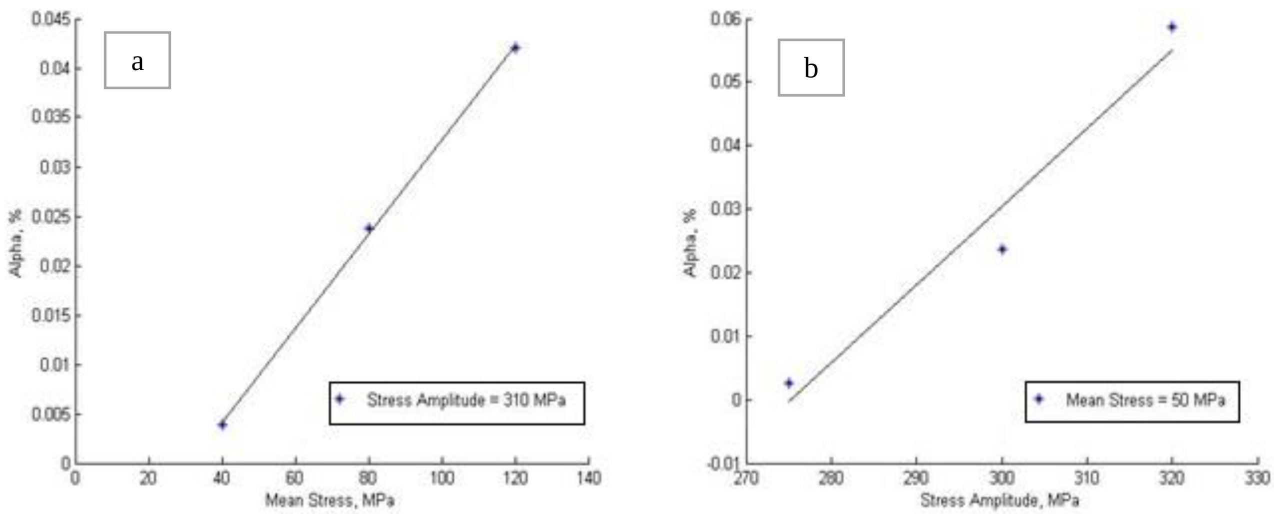

Fig. 4.8: (a) Ratcheting strain rate vs. mean stress at constant stress amplitude of 310 MPa is plotted for SA 333 Gr6C-Mn steel (b) ratcheting strain rate vs. stress amplitude at constant mean stress of 50 MPa is plotted for 20CS steel.

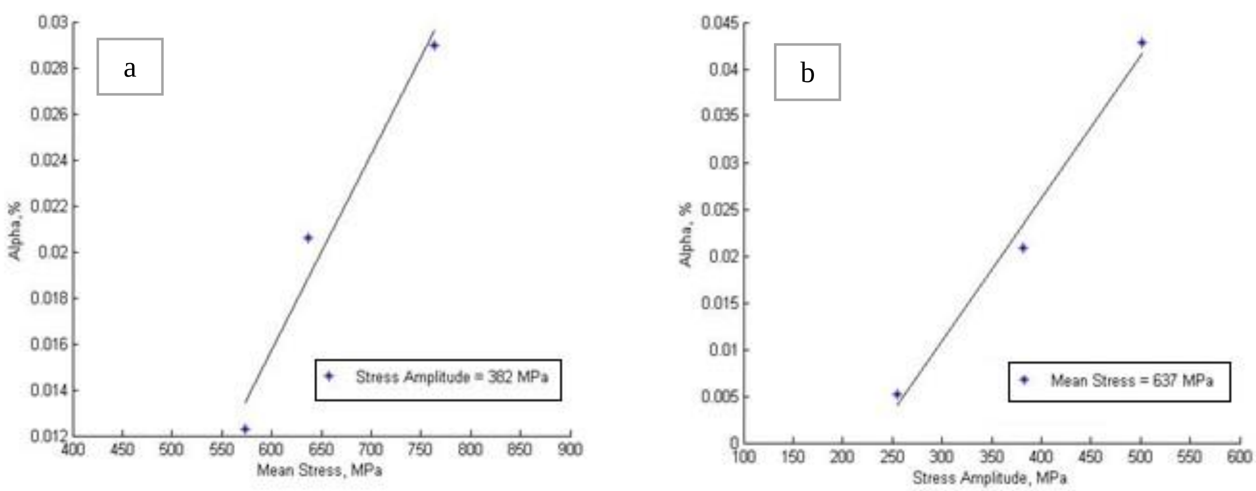

Fig. 4.9: (a) Ratcheting strain rate vs. mean stress at constant stress amplitude of 382 MPa (b) ratcheting strain rate vs. stress amplitude at constant mean stress of 637 MPa is plotted for X13CrMnMoN18-14-3 high nitrogen steel.

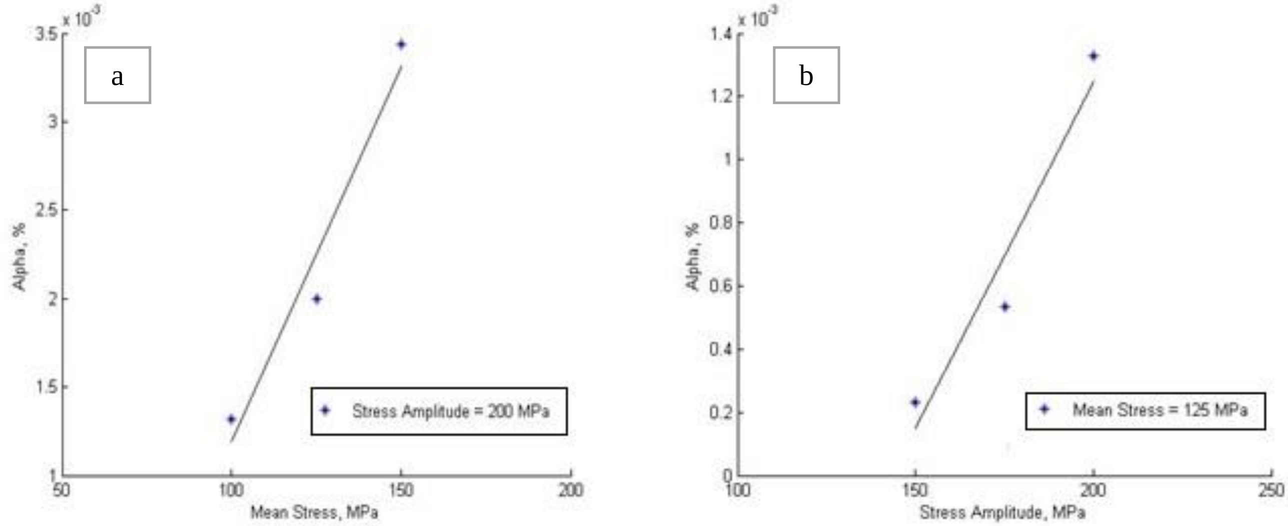

Fig. 4.10: (a) Ratcheting strain rate vs. mean stress at constant stress amplitude of 200 MPa (b) ratcheting strain rate vs. stress amplitude at constant mean stress of 125 MPa is plotted for Z2CND18-12N steel.

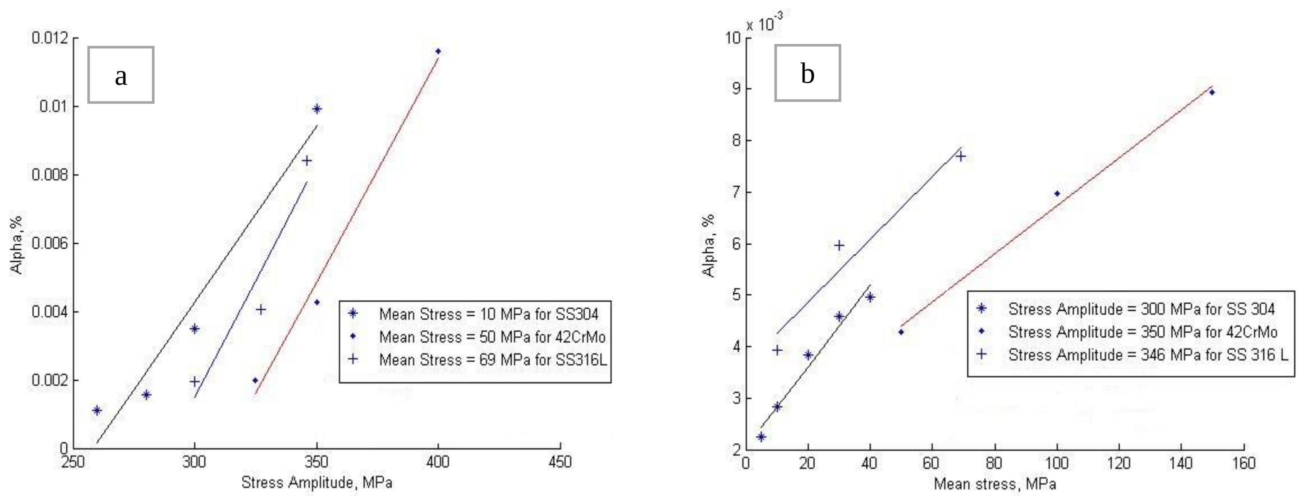

Fig. 4.11: (a) Ratcheting strain rate vs. mean stress at constant stress amplitude and (b) ratcheting strain rate vs. stress amplitude at constant mean stress is plotted for three different steel.

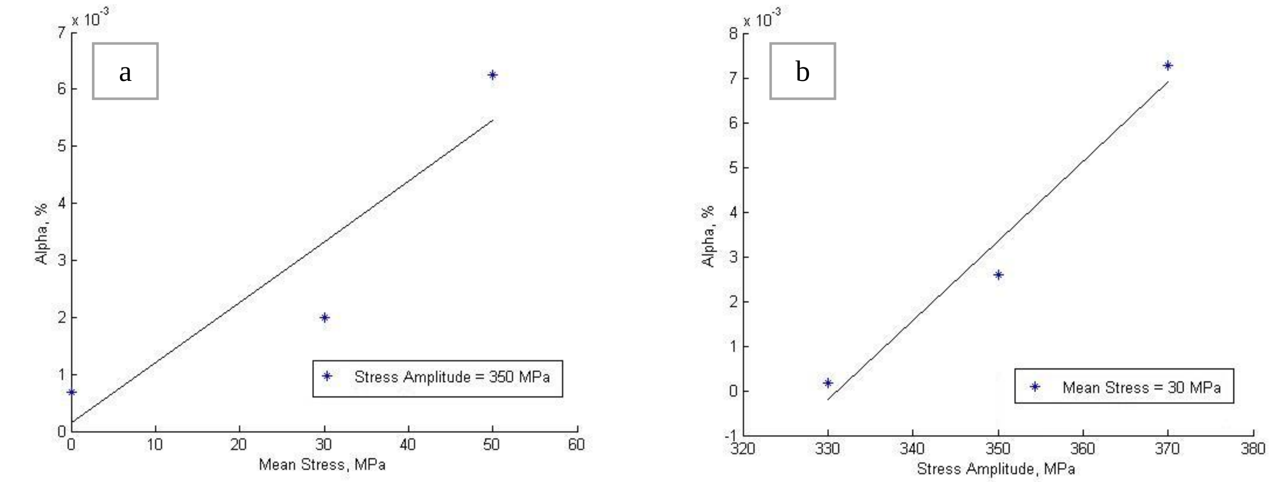

Fig. 4.12: (a) Ratcheting strain rate vs. mean stress at constant stress amplitude of 350 MPa (b) ratcheting strain rate vs. stress amplitude at constant mean stress of 30 MPa is plotted for HC340LA steel.

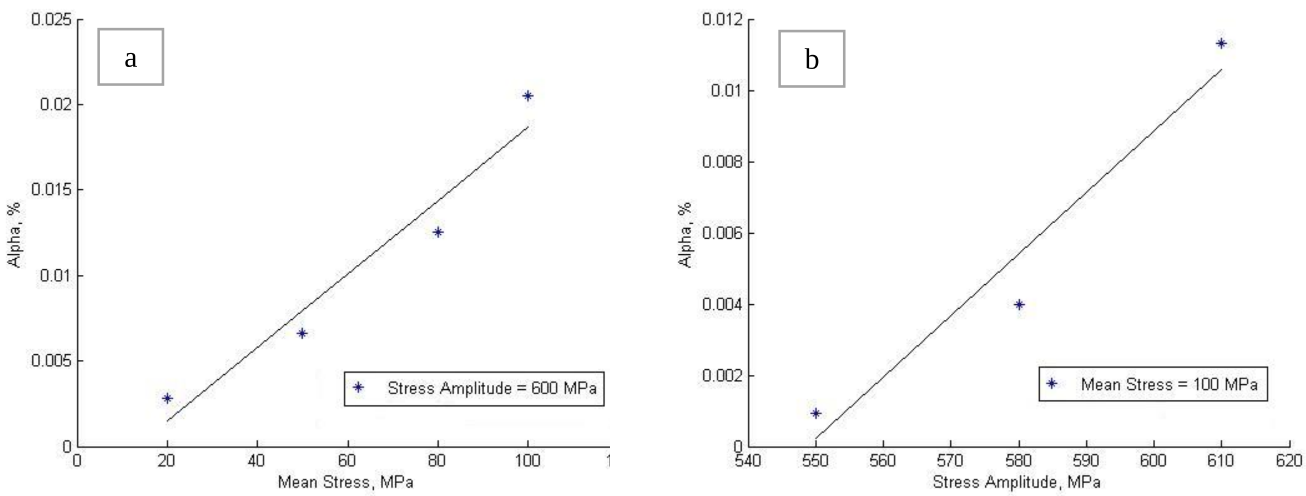

Fig. 4.13: (a) Ratcheting strain rate vs. mean stress at constant stress amplitude of 600 MPa (b) ratcheting strain rate vs. stress amplitude at constant mean stress of 100 MPa is plotted for HC340LA steel.

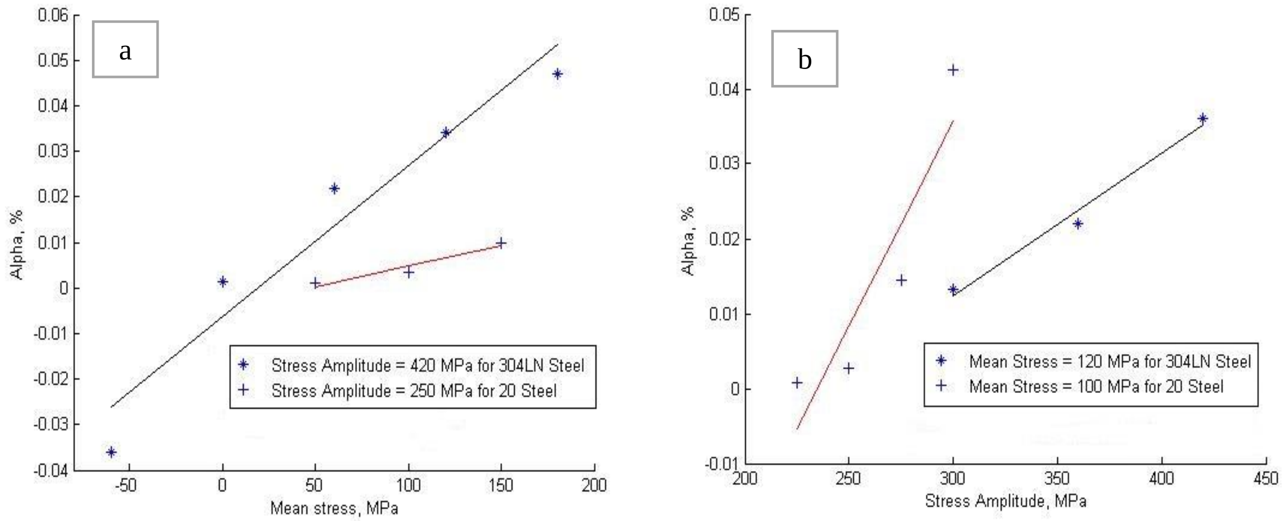

Fig. 4.14: (a) Ratcheting strain rate vs. mean stress at constant stress amplitude and (b) ratcheting strain rate vs. stress amplitude at constant mean stress of is plotted for 304LN Stainless steel and 20 Steel.

Linear fit line is drawn in for the plots shown in Fig. 4.2 to 4.14. These lines are generated using a linear equation.

$$y = m\,x + c \tag{4.2}$$

Slope m and y-intercept c are obtained from the above graphs using Matlab coding.

Using Eq. 4.2, we can find the value of mean stress and stress amplitude at zero ratcheting strain rate. The list of mean stress and stress amplitude at zero ratcheting stain rate as shown in Table 4.1.

Table 4.1: Slope, y-intercept, mean stress and stress amplitude values at zero ratcheting strain for different steels.

Material	Slope from the linear equation *m*	Y-intercepts from the linear equation *c*	Zero ratcheting strain rate ($\alpha = 0$)	
			Mean Stress (σ_m), MPa	Stress Amplitude (σ_a), MPa
16MnR Steel	0.00010814	-0.003	27.74	360
	0.000646	-0.22628	100	350.27
Interstitial Free Steel	0.0005845	0.0183133	-31.33	150
	0.000841	0.0040567	-4.823	140
	0.001093	-0.0090133	8.25	130
	0.001346	-0.1701133	10	126.38
SS304	0.000053467	0.002277156	-42.59	300
	0.0001405	-0.0372244	10	264.94
42CrMo Steel	0.0000712	-0.0010167	14.28	350
	0.000091987	-0.02738	50	297.65

Material	Slope from the linear equation *m*	Y-intercepts from the linear equation *c*	Zero ratcheting strain rate ($\alpha = 0$)	
			Mean Stress (σ_m), MPa	Stress Amplitude (σ_a), MPa
Titanium-Stabilized Free Steel	0.63454E-6	-0.0675E-6	0.106	144.2
	0.000018294	-0.0028023	28.84	153.18
42CrMo Steel Alloy	0.0000384	0.00187	-48.70	350
1020 Steel Alloy	0.009985	-0.29182	50	292.25
20CS Steel	0.00122697	-0.337712	50	275.24
SA333Gr6C-Mn Steel	0.00047637	-0.01488	31.236	310
X13CrMnMoN18-14-3 High Nitrogen Steel	0.00015242	-0.0349142	637	229.06
	0.00008443	-0.0349217	413.617	382
Z2CND18-12N Steel	0.0000424	-0.0030467	71.86	200
	0.00002194	-0.0031408	125	142.828
SS304	0.00010297	-0.0266204	10	258.525
	0.0000827085	0.00181092	-21.89	300

Material	Slope from the linear equation *m*	Y-intercepts from the linear equation *c*	Zero ratcheting strain rate ($\alpha = 0$)	
			Mean Stress (σ_m), MPa	Stress Amplitude (σ_a), MPa
42CrMo Steel	0.000130686	-0.0408757	50	312.77
	0.00004654	0.00161267	-34.65	350
SS316L	0.000136186	-0.03936339	69	289.04
	0.00060922065	0.003650165	-5.91189	346
HC340LA Steel Alloy	0.0001776	-0.05881067	30	331.14
	0.0001727	-0.0947533	100	548.66
	0.000106079	0.00014789	-1.39	350
	0.0002143395	-0.002777966	12.968	600
30LN Stainless Steel	0.0003427167	-0.007489	21.85	420
	0.000190083	-0.0452933	120	238.28
20 Steel	0.000089	-0.0041	46.07	250
	0.00054816	-0.12876699	100	234.907

From the Table 4.1 for zero ratcheting strain rate we obtain the corresponding mean stress and stress amplitude for different steel materials using the linear equation generated from the Fig. 4.2 to 4.14. The slope, m and y-intercept, c values are obtained using Matlab coding. Hence by loading the material using these mean stress and stress amplitude we can arrest the ratcheting or reduce ratcheting up to the large extent in the material. Hence, finally the material life can be increased.

4.3 Mean and amplitude stress relations

Materials are used to steady cyclic loading subjected deformation; hence the material response is studied with the help of applied mean stress and stress amplitude subjected to loading cycles. Two dimensions XY graph is plotted with stress amplitude/yield stress as X component and mean stress/yield stress as Y component. An exponential curve is drawn using Matlab coding and the corresponding equation is obtained for different steel material as listed in Table 4.2.

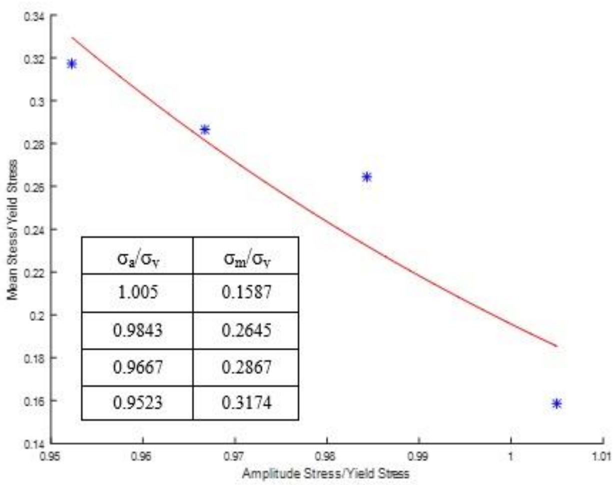

Fig. 4.15: Mean and amplitude stress relation for 16MnR steel at yield stress of 378 MPa.

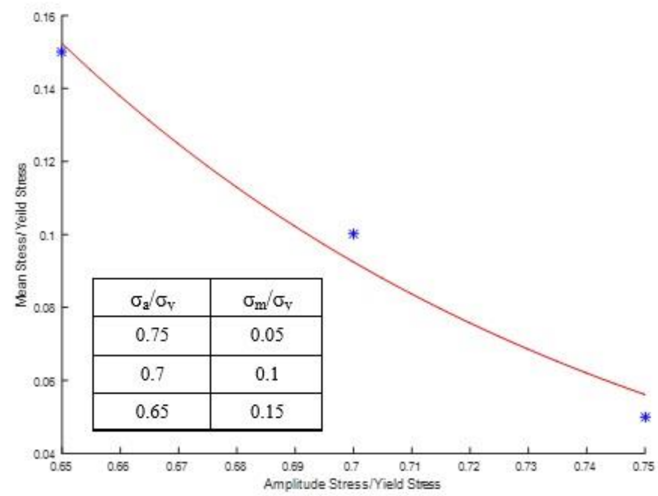

Fig. 4.16: Mean and amplitude stress relation for interstitial free steel at yield stress of 200 MPa.

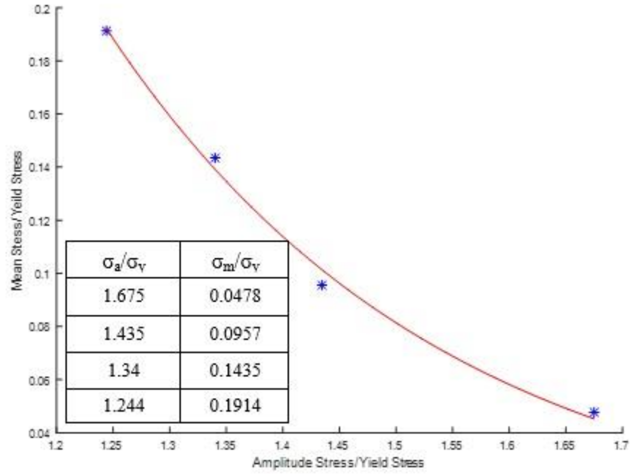

Fig. 4.17: Mean and amplitude stress relation for SS304 steel at yield stress of 209 MPa.

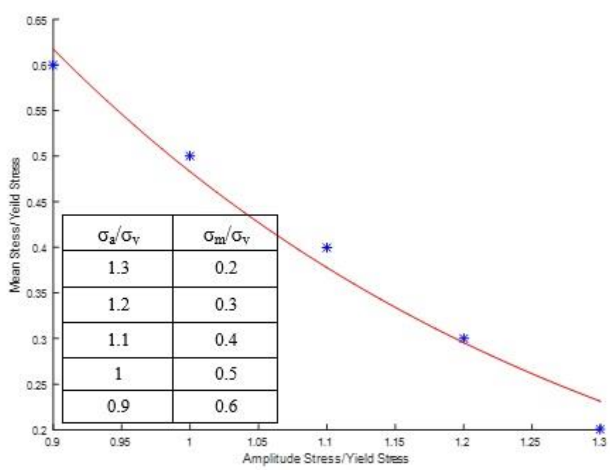

Fig. 4.18: Mean and amplitude stress relation for 42CrMo steel at yield stress of 310 MPa.

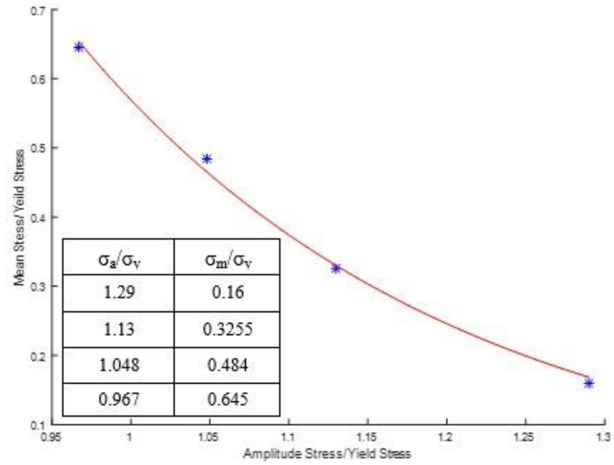

Fig. 4.19: Mean and amplitude stress relation for titanium-stabilized interstitial free steel at yield stress of 144.2 MPa.

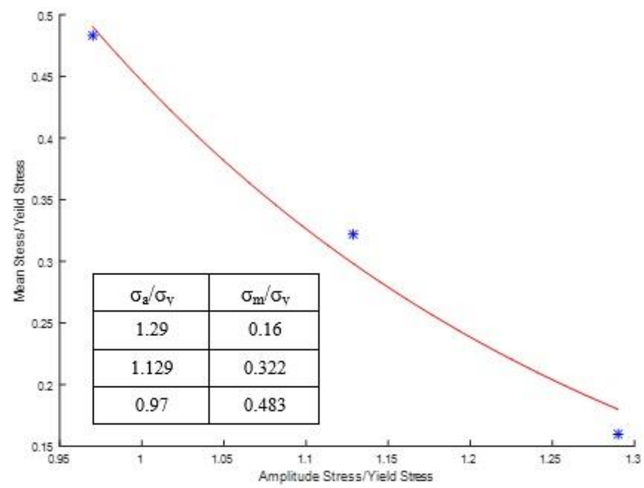

Fig. 4.20: Mean and amplitude stress relation for 42CrMo steel at yield stress of 310 MPa.

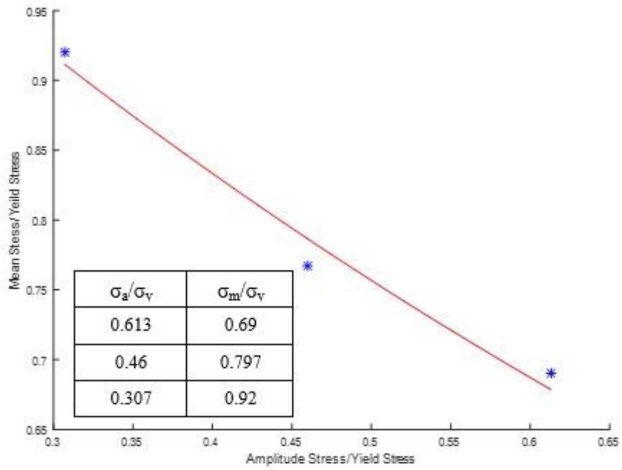

σ_a/σ_Y	σ_m/σ_Y
0.613	0.69
0.46	0.797
0.307	0.92

Fig. 4.21: Mean and amplitude stress relation for X13CrMnMoN 18-14-3 high nitrogen steel at yield stress of 830 MPa.

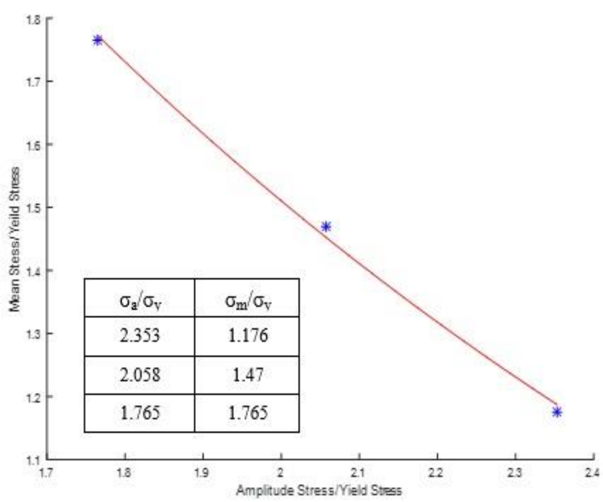

σ_a/σ_Y	σ_m/σ_Y
2.353	1.176
2.058	1.47
1.765	1.765

Fig. 4.22: Mean and amplitude stress relation for Z2CND18.12N steel at yield stress of 85 MPa.

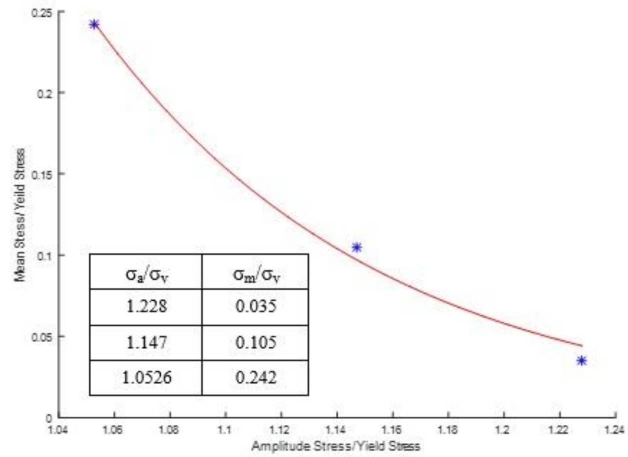

σ_a/σ_Y	σ_m/σ_Y
1.228	0.035
1.147	0.105
1.0526	0.242

Fig. 4.23: Mean and amplitude stress relation for 316L steel at yield stress of 285 MPa.

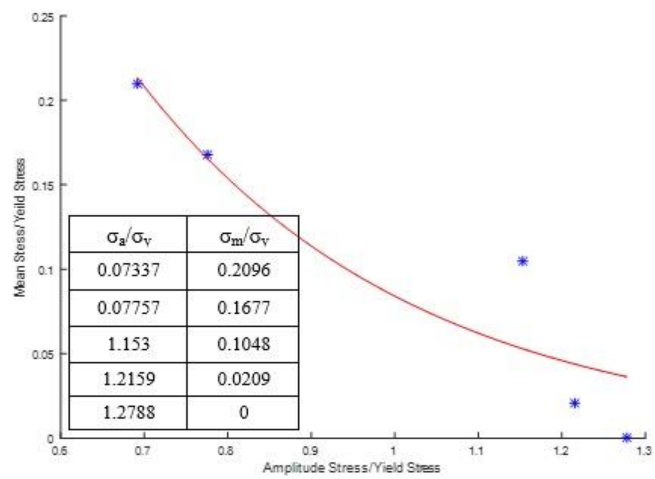

σ_a/σ_Y	σ_m/σ_Y
0.07337	0.2096
0.07757	0.1677
1.153	0.1048
1.2159	0.0209
1.2788	0

Fig. 4.24: Mean and amplitude stress relation for HC340LA steel at yield stress of 477 MPa.

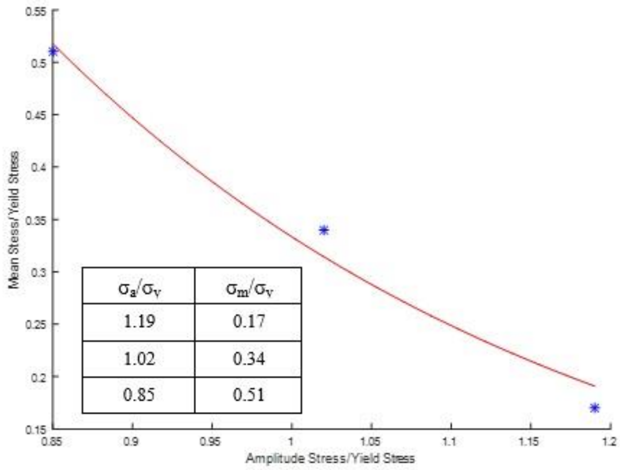

Fig. 4.25: Mean and amplitude stress relation for 304LN steel at yield stress of 353 MPa.

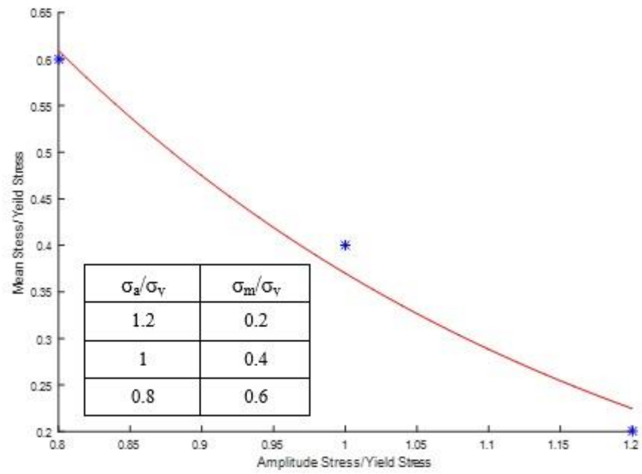

Fig. 4.26: Mean and amplitude stress relation for 20 Steel at yield stress of 250 MPa.

The exponential equation of the curve obtained in Fig. 4.15 to 4. 26 are in the form of

$$F(x) = C.e^{kx} \qquad (4.3)$$

where C and k are Constants.

Table 4.2 shows all the constants and real constants value of different material in the Fig. 4.15 – 4.26 mean and amplitude stress relation graphs.

Table 4.2: Values of the exponential equation constants in mean and amplitude stress relation graphs for different steel materials.

Material	$F(x) = C.e^{kx}$	
	Constant C	Constant k
16MnR Steel	56799	-12.63
Interstitial Free Steel	198.7	-10.99
SS304	10.734	-3.245

Material	$F(x) = C.e^{kx}$	
	Constant C	Real Constant k
42CrMo Steel	45.658	-4.375
Titanium-Stabilized Free Steel	7.3311	-2.708
42CrMo Steel Alloy	14.458	-3.455
X13CrMnMoN18-14-3 High Nitrogen Steel	1.2123	-0.94
Z2CND18-12N Steel	6.0109	-0.691
SS316L	26513	-10.98
HC340LA Steel Alloy	2.1917	-3.287
30LN Stainless Steel	8.3406	-3.233
20 Steel	0.3504	-2.677

4.4 Three dimensional ratcheting surface zone

Ratcheting three-dimensional surface zone is formulated by combining the solutions of ratcheting strain rate with constant mean stress and varying stress amplitude and also with constant stress amplitude and varying mean stress of different steel alloys from Fig. 4.27 – 4.37. The mathematical equation used to generate this three-dimensional surface is as follows

$$\alpha = (m_1.\sigma_m + m_2.\sigma_a + c_1 + c_2)/2 \quad (4.4)$$

where α = ratcheting strain rate, σ_m = mean stress, σ_a = stress amplitude, m_1 and m_2 are slope and c_1 and c_2 are y intercepts of the linear equation at constant mean stress and constant stress amplitude condition.

The result shows an irregularly inclined surface. Therefore, we can find the respective for different mean and amplitude stress graphically.

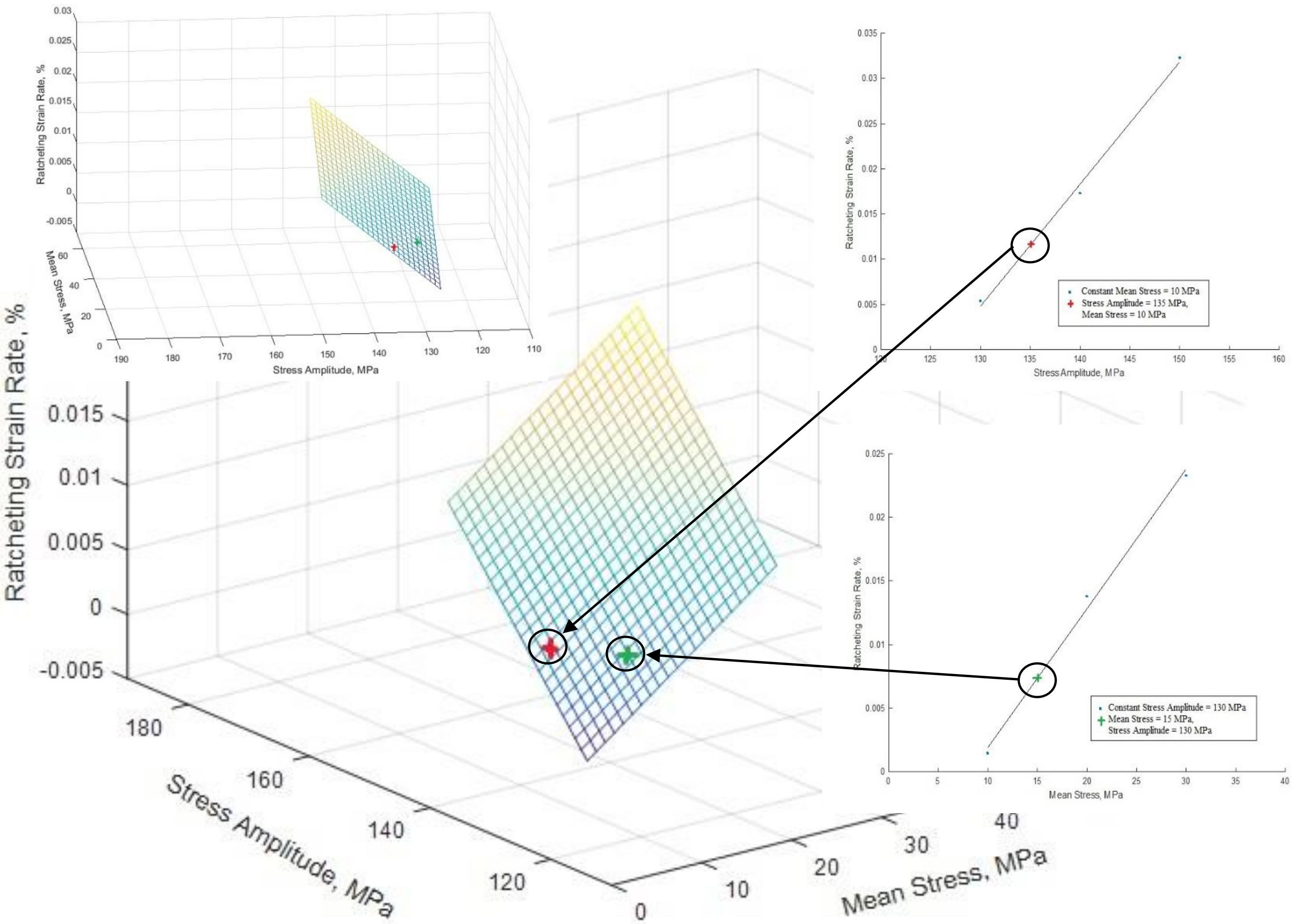

Fig. 4.27: Three dimensional ratcheting surface zone for applied stress amplitude and mean stress for interstitial free steel.

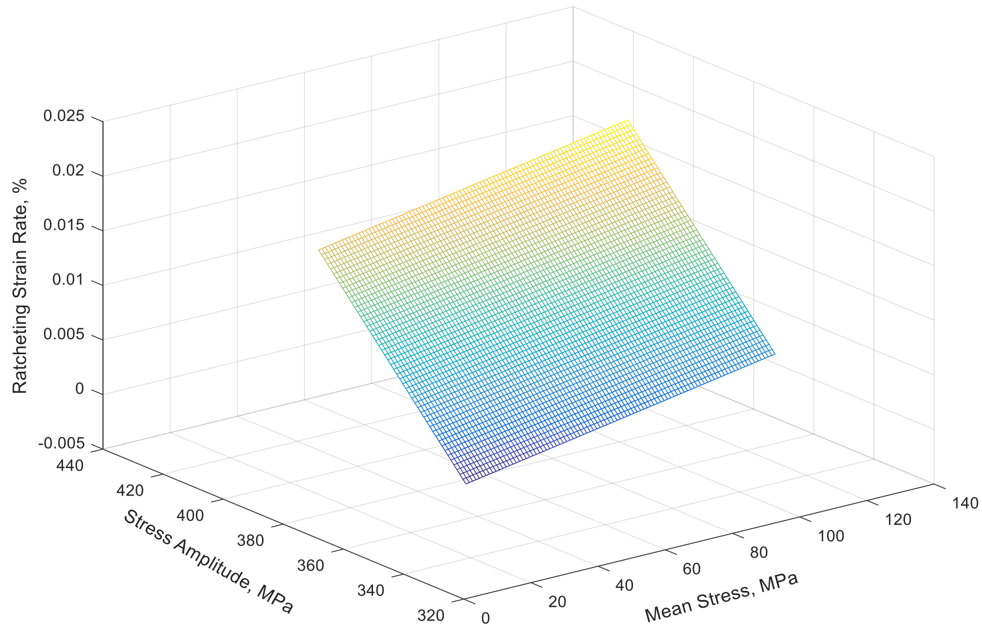

Fig. 4.28: Three dimensional ratcheting surface zone for applied stress amplitude and mean stress for 16MnR steel.

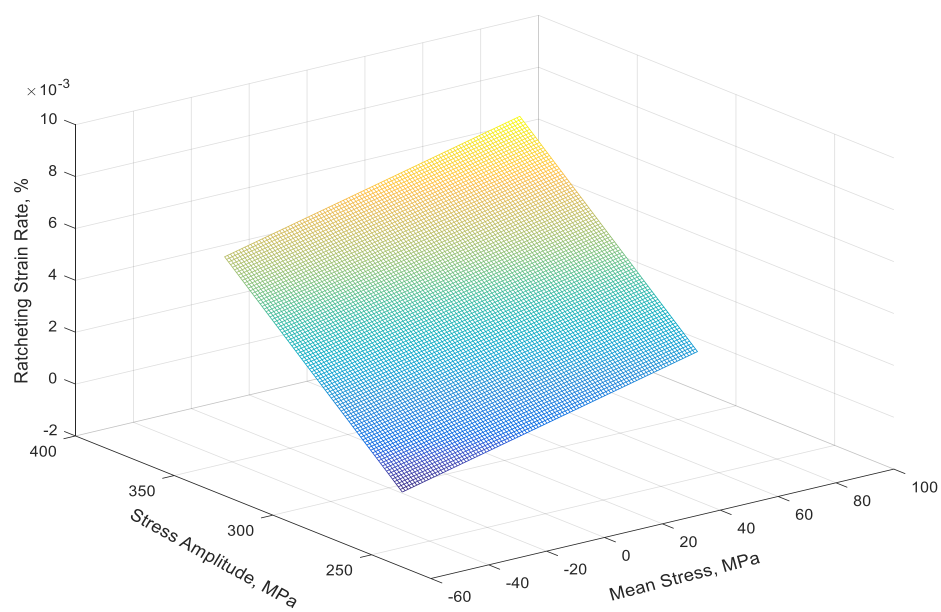

Fig. 4.29: Three dimensional ratcheting surface zone for applied stress amplitude and mean stress for SS304 stainless steel.

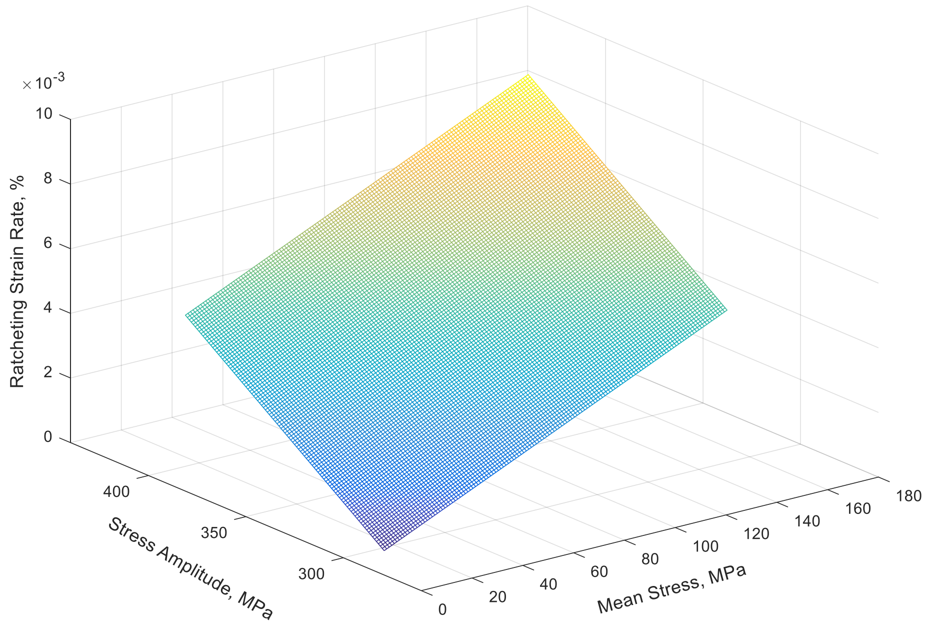

Fig. 4.30: Three dimensional ratcheting surface zone for applied stress amplitude and mean stress for 42CrMo steel.

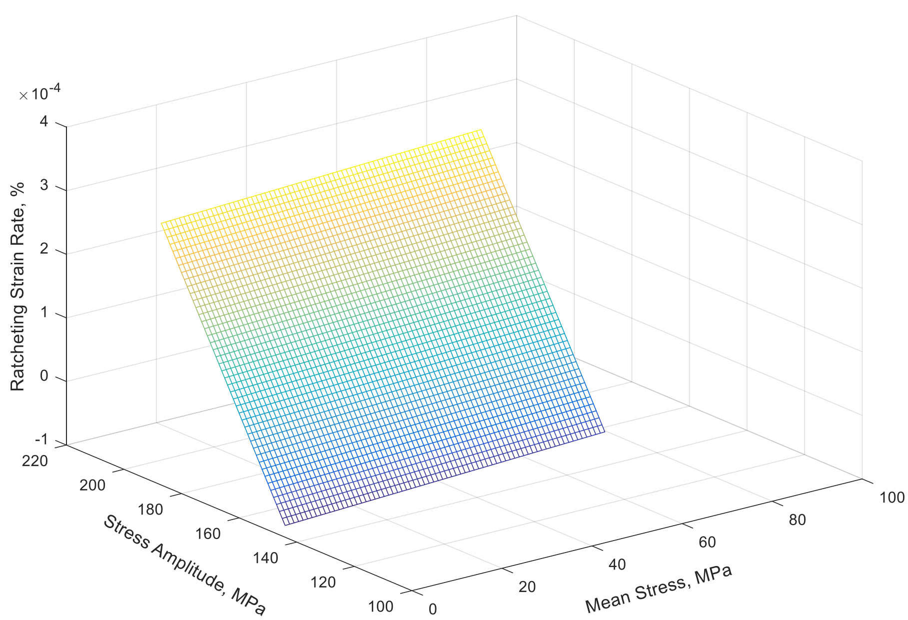

Fig. 4.31: Three dimensional ratcheting surface zone for applied stress amplitude and mean stress for titanium-stabilized free steel.

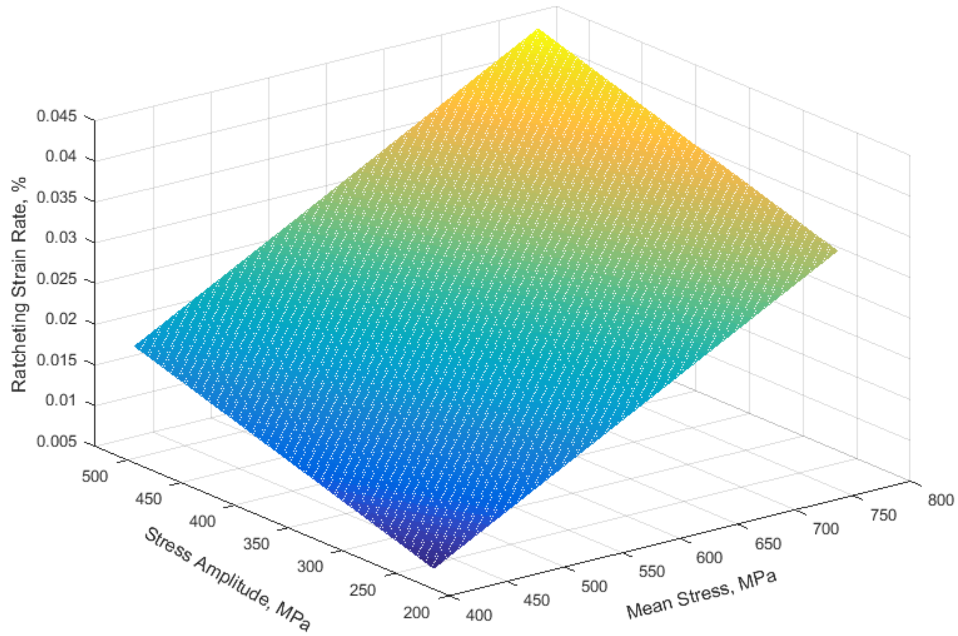

Fig. 4.32: Three dimensional ratcheting surface zone for applied stress amplitude and mean stress for X13CrMnMoN18-14-3 high nitrogen steel.

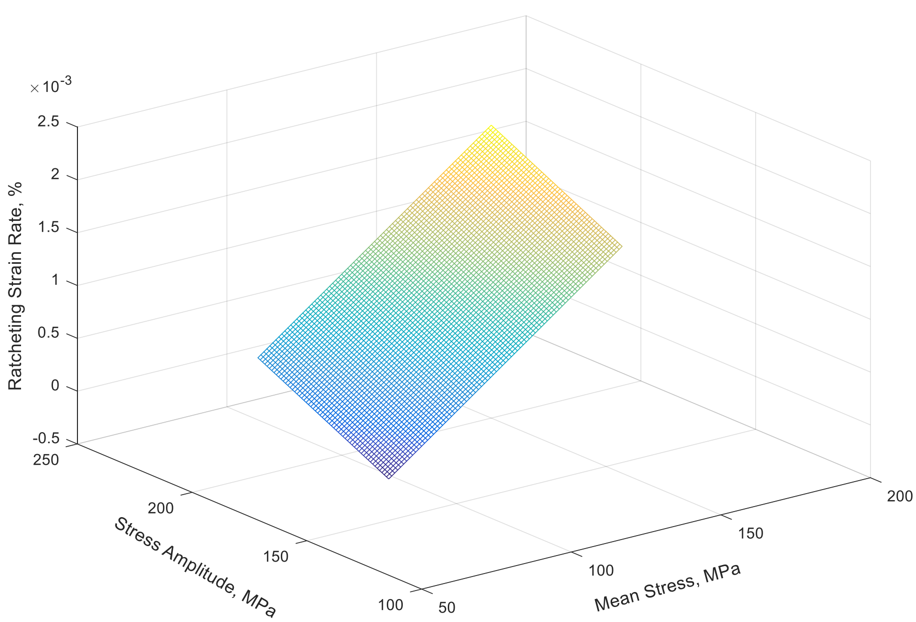

Fig. 4.33: Three dimensional ratcheting surface zone for applied stress amplitude and mean stress for Z2CND18-12N steel.

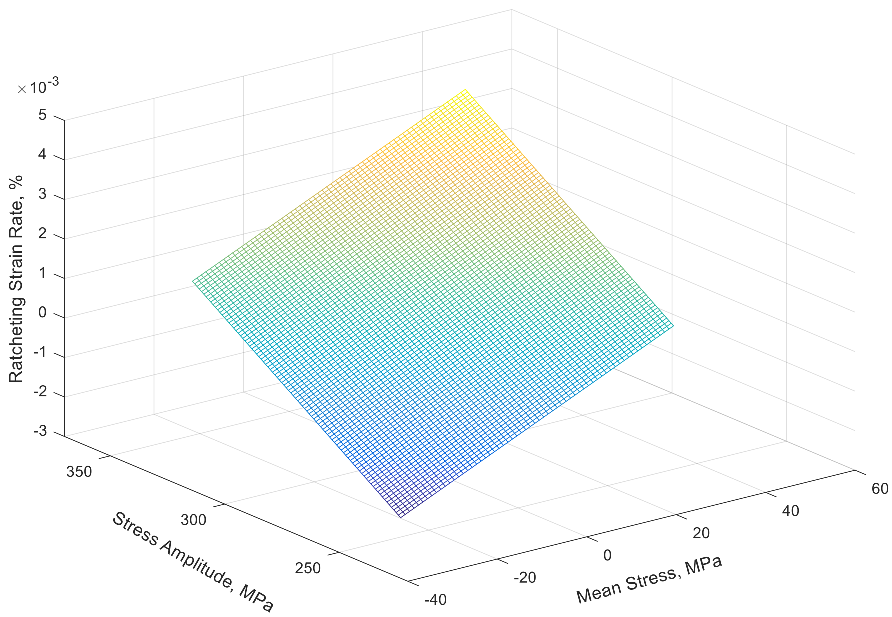

Fig. 4.34: Three dimensional ratcheting surface zone for applied stress amplitude and mean stress for SS316L steel.

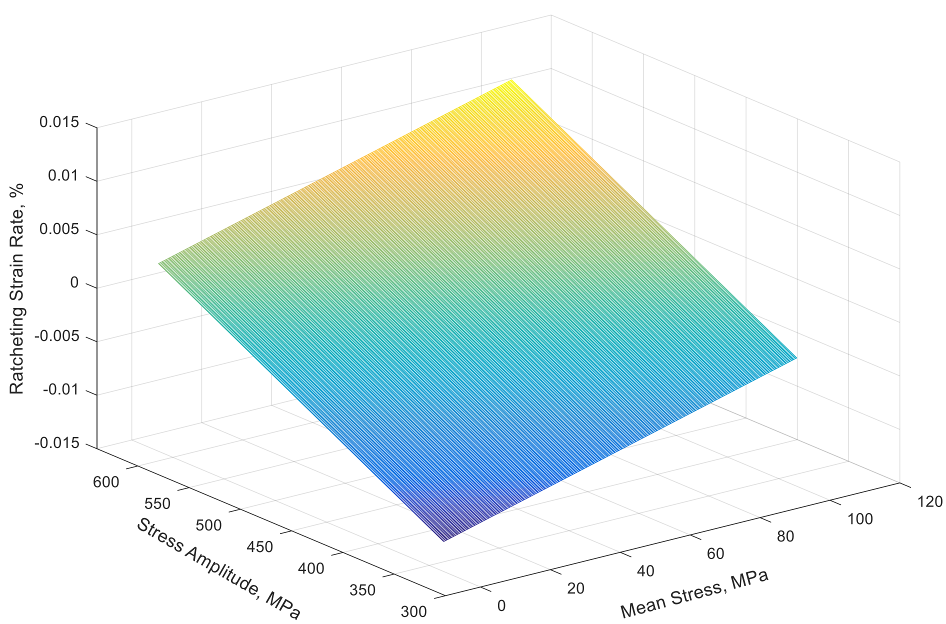

Fig. 4.35: Three dimensional ratcheting surface zone for applied stress amplitude and mean stress for HC340LA steel alloy.

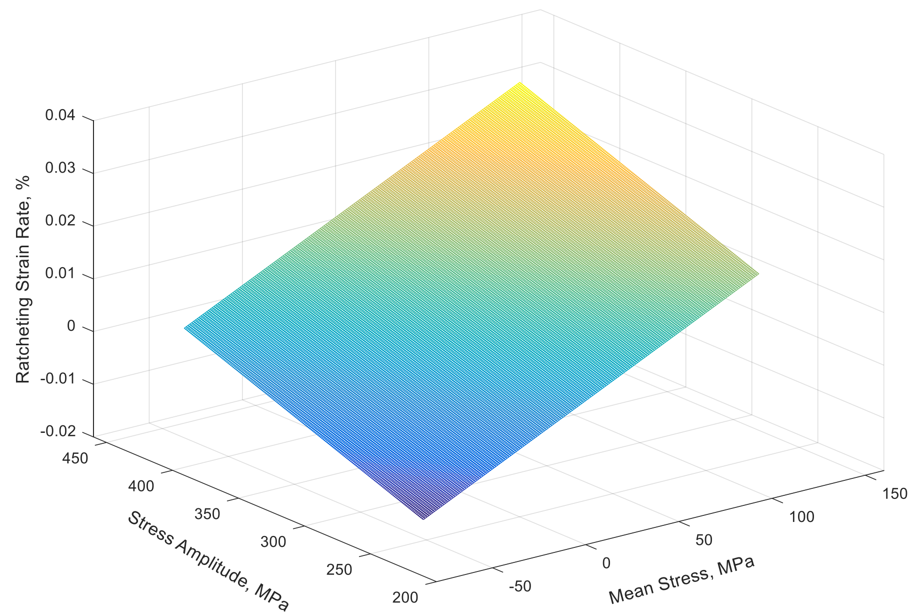

Fig. 4.36: Three dimensional ratcheting surface zone for applied stress amplitude and mean stress for 30LN stainless steel.

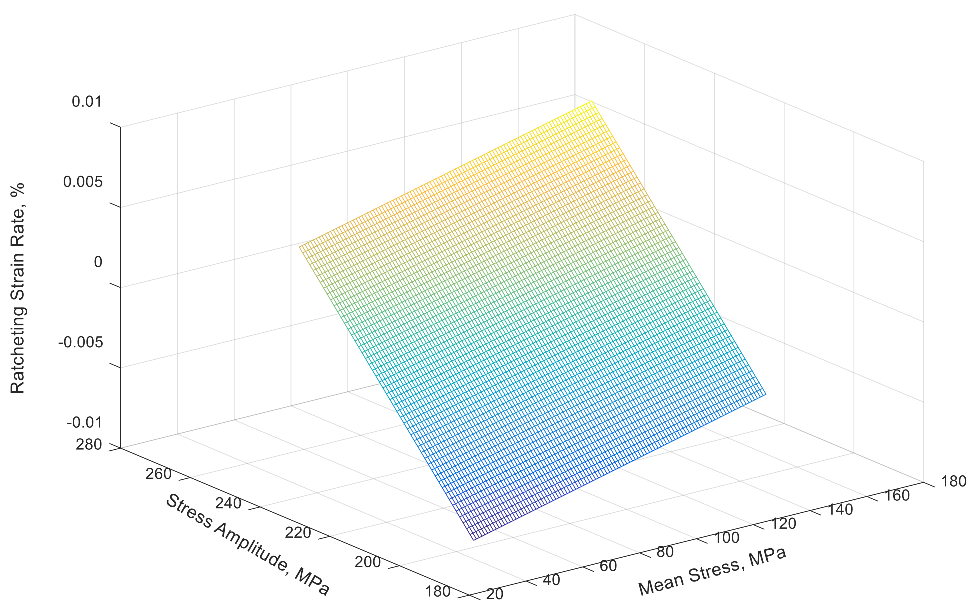

Fig. 4.37: Three dimensional ratcheting surface zone for applied stress amplitude and mean stress for 20 steel.

4.5 Overview

From Fig. 4.27 – 4.37 it can be shown that the ratcheting strain of various steel alloys can be found for different sets of applied mean and amplitude stress. The three-dimensional surface zone is constructed with certain boundary limits of maximum mean and amplitude stresses applied in the experiment. The boundaries can be increased by extending the trend line without changing the slopes and intercepts.

CHAPTER 5

Conclusion

The accumulation of ratcheting strain in different steels due to uniaxial loading is found to increase if the magnitude of mean stress increases with constant stress amplitude condition. The ratcheting strain increases with an increase in the magnitude of stress amplitude with constant mean stress state. Cyclic damage in the material increases with an increase in strain accumulation that is illustrated by the hysteresis loop shifting towards the large plastic strain amplitude; due to this ratcheting phenomenon dislocation density in samples increases.

The process of ratcheting can be evaluated in three stages, in stage I ratcheting strain rate decreases with increase in the loading cycles. In stage II ratcheting strain rate reaches a constant with further increase in cycles and during this stage only ratcheting strain keeps on growing at a steady rate. In the final stage, ratcheting strain rate increases drastically until the failure occurs. Hence from Table 2.1 we can conclude that ratcheting can be arrested and cannot be increased further if the material is loaded under zero ratcheting strain rate condition with specified mean stress and stress amplitude.

The three dimensional ratcheting surface is formulated for different steel materials to study the ratcheting behavior of those materials under various combinations of mean and amplitude stresses. These graphs are expressed with the help of experimental results of certain sets of mean and stress amplitude conditions. Multiple sets of stress combinations and their corresponding ratcheting rate can be obtained with some limited sets of experimental results. As a consequence, experimentation cost and time can be saved.

REFERENCES

[1] C. Li, G. Chen, X. Chen and W. Zhang. Ratcheting strain and stimulation of 16MnR steel under uniaxial cyclic loading. Computational material science 57 (2012) 43-47.

[2] K. Dutta and K.K. Ray. Ratcheting Strain in interstitial free steel. Materials science and engineering A575 (2013) 127-135.

[3] G. Kang, Y. Liu and Z. Li. Experimental study on ratcheting-fatigue interaction of SS304 stainless steel in uniaxial cyclic loading. Material science and engineering A 435-436 (2006) 396-404.

[4] G. Kang and Y. lie. Uniaxial ratcheting and low-cycle fatigue failure of the steel with cyclic stabilizing or softening feature. Material science and engineering A 472 (2008) 258-268.

[5] P.S. De, P.C. Chakraborti, B. Bhattacharya, M. Shome and D.Bhattacharjee. Ratcheting behavior of titanium-stabilized interstitial free steel. Metallurgical and materials transactions 44(5) (2013) 2106-2120.

[6] G.R. Ahmadzadeh and A. Varvani-Farahani. Ratcheting assessment of steel alloys under uniaxial loading: a parametric model versus hardening rule of bower. Fatigue and fracture engineering materials and structures 36(4) (2013) 281-292.

[7] K. Dutta, L. Sahu and A. K. Mishra. Ratcheting behavior of non-conventional stainless steel and associated microstructural variations. JMEPEG 23(11) (2014) 4122-4129.

[8] G.R. Ahmadzadeh and A. Varvani-Farahani. Triphasic ratcheting strain prediction of material over stress cycles. Fatigue and fracture of engineering material and structures 35(10) (2012) 929-935.

[9] G. Chen, X. Chen and C. Niu. Uniaxial ratcheting behavior of 63Sn37Pb solder with loading histories and stress rates. Material science and engineering A 421(1) (2006) 238-244.

[10] G. Chen, S. Shan, X. Chen and H. Yuan. Ratcheting and fatigue properties of the high-nitrogen steel X13CrMnMoN18-14-3 under cyclic loading. Computational material science 46(3) (2009) 572-578.

[11] D. Yu, G. Chen, W. Yu, D. Li and X. Chen. Visco-plastic constitutive modeling on ohno-wang kinematic hardening rule for uniaxial ratcheting behavior of Z2CND18.12N steel. International journal of plasticity 28(1) (2012) 88-101.

[12] G.R. Ahmadzadeh and A.Varvani-Farahani. Ratcheting assessment of materials based on the modified Armstrong-frederick hardening rule at various uniaxial stress levels. Fatigue and fracture of engineering materials and structures 36(12) (2013) 1232-1245.

[13] V.D. Palma, A. Tomasella, F. Frendo, C.M. Sonsino and T. Melz. Experimental analysis of the ratcheting behavior of linear flow split flanges of HC340LA. International journal of fatigue 64 (2014) 121-130.

[14] G. Kang, Y. Liu and Q. Gao. Uniaxial ratchetting-fatigue interaction of tempered 42CrMo steel and its failure model. Advanced materials research 33-37 (2008) 115-120.

[15] P.P. Dey, N. Khutia, S. Sivaprasad and S. Tarafder. Development of new cyclic plasticity model for 304LN stainless steel through simulation and experimental investigation. Mechanics of materials 78 (2014) 85-101.

[16] Y. Liu, Y. Dong, G. Kang, H. Wang, X. Cheng. Experimental study on uniaxial ratcheting of 20 steel with high number of cycles at room temperature. Acta metallurgica sinica 45(7) (2009) 826-829.

[17] G.R. Ahmadzadeh, S.M. Hamidinejad and A. Varvani-Farahani. Ratcheting prediction of 1070 and 16MnR steel alloys under uniaxial asymmetric stress cycles by means of Ohno-Wang and Ahmadzadeh-Varvani kinematic hardening rules. Journal of pressure vessel technology 137(3) (2015) 031001-1.

APPENDIX A

Mechanical Properties of materials

Table A.1 Mechanical properties of different steel alloys

Material	Young's Modulus (MPa)	Yield Stress (MPa)	Ultimate Stress (MPa)	Elongation (%)	Poisson's Ratio
16MnR Steel	2.1 E^5	378	582	27	0.28
Interstitial Free Steel	1.62 E^5	200	330	36	0.27
42CrMo Steel	1.905 E^5	310	670	15	0.28
Titanium-Stabilized Interstitial Free Steel	1.34 E^5	144.2	276.16	26.98	0.27
SS304	1.9 E^5	209	475	60	0.29
X12CrMnNiN17-7-5 Steel	1.7 E^5	154	231	45	0.27
20CS Steel	2.03 E^5	350	441	28	0.3
X13CrMnMoN18-14-3 High Nitrogen Steel	2 E^5	830	1150	40	0.29
Z2CND18.12N Steel	1.95 E^5	85	165	38	0.3
316L Steel	1.9 E^5	285	480	40	0.265
HC340LA Steel	1.76 E^5	477	488	18	0.28
304LN Stainless Steel	2 E^5	353	671	52.8	0.29
20 Steel	1.85 E^5	250	380	45	0.28

APPENDIX B

Ratcheting strain rate of materials

Table A.2 Experimental values of ratcheting strain rate in different steel alloys

Material	Mean Stress, MPa	Stress Amplitude, MPa	Ratcheting Strain Rate, %	Figures
16MnR steel	60	360	0.00355	4.2
	100		0.00763	
	120		0.0101	
	100	360	0.00628	
		380	0.0192	
interstitial free steel	10	130	0.00144	4.3
	20		0.0138	
	30		0.0233	
	10	140	0.0208	
	20		0.0265	
	30		0.0289	
	10	150	0.0331	
	20		0.0337	
	30		0.035	
	10	130	0.00538	
		140	0.0173	
		150	0.0323	
SS304 stainless steel	5	300	0.00192	4.4
	10		0.00273	
	20		0.00348	
	30		0.00397	
	40		0.00415	
	60		0.00529	
	10	260	0.00112	
		280	0.00181	
		300	0.00364	
		350	0.01257	
42CrMo steel	50	350	0.00263	4.5
	100		0.00593	
	150		0.00975	

Material	Mean Stress, MPa	Stress Amplitude, MPa	Ratcheting Strain Rate, %	Figures
42CrMo steel	50	300	0.000971	4.5
		325	0.002174	
		350	0.00308	
		400	0.01	
titanium-stabilized steel	43.26	144.2	0.00264	4.6
	57.68		0.00385	
	72.1		0.00447	
	28.84	158.62	0.00795	
		173.04	0.04035	
		187.48	0.06075	
1020 steel	100	350	0.00571	4.7
	150		0.00763	
	50	320	0.0277	
		300	0.00773	
SA 333 Gr6C-Mn steel	40	310	0.00389	
	80		0.0238	
	120		0.042	
20CS steel	50	275	0.00265	4.8
		30	0.01375	
		320	0.0586	
X13CrMnMoN18-14-3 high nitrogen steel	573	382	0.0123	4.9
	637		0.0206	
	764		0.029	
	637	255	0.005143	
		382	0.02086	
		509	0.04286	
Z2CND18-12N steel	100	200	0.00312	4.10
	125		0.002	
	150		0.00344	

Material	Mean Stress, MPa	Stress Amplitude, MPa	Ratcheting Strain Rate, %	Figures
Z2CND18-12N steel	125	150	0.000233	4.10
		175	0.000533	
		200	0.00133	
SS304 Steel	5	300	0.002242	4.11
	10		0.002826	
	20		0.00383	
	30		0.004587	
	40		0.004954	
	10	260	0.001095	
		280	0.001552	
		300	0.003496	
		350	0.00991	
42CrMo Steel	50	350	0.004286	
	100		0.006974	
	150		0.00894	
	50	325	0.002	
		350	0.00426	
		400	0.0116	
SS316L Steel	10	346	0.00394	
	30		0.005961	
	69		0.00769	
	69	300	0.001959	
		327	0.00404	
		346	0.00842	
HC340LA steel	0	350	0.00068	4.12
	30		0.002	
	50		0.00625	

Material	Mean Stress, MPa	Stress Amplitude, MPa	Ratcheting Strain Rate, %	Figures
HC340LA steel	30	330	0.000182	4.12
		350	0.00258	
		370	0.007286	
	20	600	0.002783	4.13
	50		0.00662	
	80		0.01257	
	100		0.0205	
	100	550	0.000938	
		580	0.0046	
		610	0.0113	
304LN Stainless steel	-60	420	-0.0361	4.14
	0		0.00147	
	60		0.0218	
	120		0.0341	
	180		0.047	
	120	300	0.0133	
		360	0.022	
		420	0.03611	
20 Steel	50	250	0.0011	
	100		0.0033	
	150		0.01	
	100	225	0.00083	
		250	0.00267	
		275	0.0144	
		300	0.0426	

APPENDIX C

MATLAB code to generate plots for ratcheting strain rate vs. mean stress

Example of MATLAB code used to generate plots and linear fit line for ratcheting strain rate vs. mean stress at constant stress amplitude and ratcheting strain rate vs. stress amplitude at constant mean stress.

```
clear all;
clc;
format long
x=[10;20;30];
y=[0.00144;0.0138;0.0233];
x1=[10;20;30];
y1=[0.01208;0.02165;0.0289];
x2=[10;20;30];
y2=[0.02331;0.0317;0.035];
hold on
plot(x,y,'*')
plot(x,y1,'.')
plot(x,y2,'+')
a=polyfit(x,y,1)
b=polyfit(x,y1,1)
c=polyfit(x,y2,1)
plot(x,polyval(a,x),'k-');
plot(x1,polyval(b,x1),'r-');
plot(x2,polyval(c,x2),'g-');
set(gca,'xlim',[0;40])
grid off
```

APPENDIX D

MATLAB code used to generate plots for mean stress vs. amplitude stress

Example of MATLAB code used to generate plots and exponential fit line for ratcheting mean stress/yield stress vs. stress amplitude/yield stress

```
clear all;
clc;
format long
x=[1.2;1;0.8];
y=[0.2;0.4;0.6];
hold on
f=fit(x,y,'exp1')
plot(f,x,y)
ylabel('Mean Stess/Yeild Stress')
xlabel('Amplitude Stress/Yield Stress')
grid off
```

APPENDIX E

MATLAB code used to generate three dimensional surface

Example of MATLAB code used to generate three dimensional surface where mean stress as x axis, stress amplitude as y axis and ratcheting strain rate as z axis

```
clear all;
clc;
x=[10;20;30;10;10;10;8.25;10];
y=[130;130;130;130;140;150;130;126.28];
[x,y]=meshgrid(8.25:30,126.28:150)
z=(0.0005465*x)+(0.000673*y)-0.0895633;
figure
mesh(x,y,z)
set(gca,'xlim',[0;70])
set(gca,'ylim',[110;190])
hold on
```